vitro and in vivo.[14,15] We also found that wt-*p53* gene transfer could promote bystander effects to neighboring tumor cells through the multiple mechanisms, including antiangiogenesis and neutrophil-mediated immune responses.[16,17]

On the basis of these promising preclinical results, a multi-institutional, dose-escalation phase I study of ADVEXIN was conducted in Japanese patients with advanced NSCLC who had failed conventional treatments such as chemotherapy and radiotherapy. We assessed the tolerability of repeated administration of ADVEXIN for more than 6 months, which was not examined in previous phase I and II trials in the United States.[18-20]

PATIENTS AND METHODS

Patient Eligibility

Patients were included who met the following criteria: between 15 and 75 years old; histologically confirmed advanced NSCLC, resistant or refractory to standard therapies; lesions accessible for repeated injection; measurable disease; Zubrod performance status of 2 or lower; life expectancy greater than 12 weeks; and adequate bone marrow, liver, and renal function. Pretreatment tumor biopsies must show a *p53* mutation by single-strand conformation polymorphism analysis.

Study Design

The protocol was approved by the institutional review board of the participating institutions as well as by the Ministry of Health and Welfare. The trial was a multicenter, open-label, phase I dose-escalation study of ADVEXIN. Six patients were treated per dose level, starting with a dose of 1×10^9 plaque-forming units (PFU; 2×10^{10} virus particles) and escalating in log increments to a maximal dose of 1×10^{11} PFU (2×10^{12} virus particles). Initially, three patients were treated with ADVEXIN as monotherapy at each dose level. If no toxicity was observed with the vector, then the next three patients received ADVEXIN in combination with intravenous administration of cisplatin. In a cohort of 1×10^{11} PFU, only three patients were treated with ADVEXIN alone because of the modification of the protocol. As many new drugs including taxanes, irinotecan, and vinorelbine became available in Japan during this trial, and cisplatin was no more a sole key drug for NSCLCs, the protocol was modified.

Treatment Plan

The construction and generation of ADVEXIN was reported previously.[9,14,21] The vector was injected directly into the primary tumor, either endobronchially using a bronchoscope or percutaneously under computed tomography (CT) guidance. For lesions of at least 4 cm in the largest diameter, the final volume administered was 10 mL; for lesions with a diameter of less than 4 cm, the final volume injected was 3 mL. In the cohorts with ADVEXIN plus cisplatin, patients were treated intravenously with 80 mg/m^2 of cisplatin on day 1 and study vector injected intratumorally on day 4. Treatments were repeated every 28 days.

Toxicity and Response Criteria

Patients were monitored with regard to safety and tolerability according to the National Cancer Institute's Common Toxicity Criteria (version 2) for a minimum of 12 months or until death. Indicator lesions were measured serially by bronchoscope or radiographic scanning, and underwent biopsy for histology and molecular analyses. Standard response criteria were used to evaluate target tumor response.

Determinations of Antibody Titer

Serum samples were collected at baseline and before each course of treatment, and tested for the presence of neutralizing antiadenovirus antibody and anti-p53 antibody. Neutralizing antibodies to Ad5 were detected by their ability to inhibit the cytopathic effect (CPE) of adenovirus on 293 cells. The mixture of an Ad5 suspension and diluted plasma was applied to a monolayer of 293 cells in 96 well plates. The cells were incubated until the appearance of CPE. The titer of neutralizing antibodies in plasma was equivalent to the inverse value of the dilution at which 100% of the CPE was observed. The titers of anti-p53 antibodies were tested by means of a qualitative enzyme-linked immunosorbent assay kit.

Analysis of Tumor Biopsy Tissues

Pretreatment (immediately before) and post-treatment (48 hours after) tumor biopsy specimens were obtained by core biopsies of the vector-injected tumor after each course of treatment. Tissue samples were also used for conventional reverse-transcriptase polymerase chain reaction (RT-PCR) assay to detect expression of exogenous p53. Total RNA was isolated from frozen biopsy samples and used as a template. After RT, a nested PCR procedure was used, with vector-specific primers. mRNA copy numbers of exogenous p53, p21, Noxa, p53AIP1, and *β-Globin*, the housekeeping gene, were also determined by real-time quantitative RT-PCR using a LightCycler instrument (Roche Diagnostics, Mannheim, Germany), a LightCycler DNA Master SYBR Green I kit (Roche Diagnostics), and LightCycler-Control Kit DNA (Roche Diagnostics). All expression levels were normalized to that of β-Globin.

Analysis of Vector Dissemination and Biodistribution

ADVEXIN shedding was monitored in the gargle, urine, and plasma specimens by a vector-specific DNA-PCR assay or the CPE assay. DNA was isolated from samples and analyzed for the presence of vector DNA by PCR. The vector-specific primers were used to detect p53 open-reading-frame/adenoviral DNA junction. The CPE assay is a bioassay to semiquantitatively detect the amount of vector contained in a biologic fluid.

RESULTS

Patient Characteristics

Fifteen patients with advanced NSCLC who had failed prior conventional therapies were enrolled onto this clinical trial from February 1999 to April 2003 (Table 1). Patients were primarily male (14 males and 1 female), with median age of 58 years (range, 46 to 71 years). Nine patients (60%) had prior chemoradiotherapy and six patients (40%) had prior chemotherapy. Fourteen patients (93.3%) were treated with platinum-based regimens containing either cisplatin or carboplatin. The median number of courses per patient was three (average, 4.2), and the range was one to 14 courses.

Adverse Events

Toxicities and adverse events (AE) that occurred in all patients are presented in Table 2. Among the 15 treated patients, none withdrew from the study as a result of toxicity, and no grade 4 toxicities classified as being possibly, probably, or definitely related to the vector were observed. The most frequent vector-related AE was a transient fever. In most patients (93.3%), self-limited fever developed 6 to 24 hours after ADVEXIN injection regardless of dose, with a highest reported grade of 3. Patients generally recovered within 48 hours, although four patients (26.7%; patients 3, 7, 8, and 13) developed grade 2 or 3 obstructive pneumonia categorized as not related or probably not related to study medication. Hematologic toxicity was limited, with one incidence of grade 1 leukopenia (6.7%) and three incidences of grade 2 or 3 anemia (20%). Transient, mild increases in liver ALT and AST were noted in one patient treated with ADVEXIN alone. Liver enzymes recovered to pretreatment values within 10 days.

Clinical Outcome

Thirteen of 15 patients (86.7%) were assessable for response with CT scan, broncoscopic, and clinical findings. Objective responses were a partial response in one patient (7.7%), stable disease (SD) in 10 patients (76.9%), and progressive disease in two patients (15.4%; Table 1). The median time of SD was 4.4 months (range, 1 to 11

Table 1. Characteristics of Patients and Tumors Who Received Injections of ADVEXIN,* and Response of Injected Lesion

Patient No.	Sex	Age (years)	Histology	Location of Tumor	Prior Therapy	TNM Stage	Method of Injection	Viral Dose + Cisplatin	No. of Courses	Response
1	Male	58	Squamous	Carina	Chemotherapy; radiotherapy	cT4N0M0 stage IIIB	Bronch	10^9 PFU	14	PR
2	Male	58	Squamous	Left lower lobe	Chemotherapy; radiotherapy	cT4N2M0 stage IIIB	Bronch; CT	10^9 PFU	9	SD
3	Male	66	Squamous	Right mainstem bronchus	Surgery, laser; chemotherapy	cT2N0M0 stage IB; (pre-operative)	Bronch	10^9 PFU	4	PD
4	Female	46	Adeno	Left upper lobe	Chemotherapy	cT2N3M1 stage IV	CT	10^9 PFU + cisplatin	10	SD
5	Male	55	Squamous	Right lower lobe	Chemotherapy	cT4N1M0 stage IIIB	Bronch; CT	10^9 PFU + cisplatin	3	SD
6	Male	54	Squamous	Left upper lobe	Chemotherapy; radiotherapy	cT3N2M0 stage IIIB	CT	10^9 PFU + cisplatin	2	SD
7	Male	71	Squamous	Left upper lobe	Chemotherapy; radiotherapy	cT4N1M0 stage IIIB	Bronch	10^{10} PFU	2	PD
8	Male	52	Squamous	Right lower lobe	Chemotherapy; radiotherapy	cT2N2M0 stage IIB	Bronch	10^{10} PFU	1	Not assessable†
9	Male	66	Squamous	Left upper lobe	Surgery, laser; chemotherapy	cT2N0M0 stage IB; (pre-operative)	CT	10^{10} PFU	4	SD
10	Male	51	Adeno	Right lower lobe	Chemotherapy	cT2N2M1 stage IV	CT	10^{10} PFU + cisplatin	1	SD
11	Male	51	Adeno	Right upper lobe	Chemotherapy	cT4N3M0 stage IIIB	CT	10^{10} PFU + cisplatin	2	SD
12	Male	61	Squamous	Right upper lobe	Chemotherapy; radiotherapy	cT4N2M0 stage IIIB	Bronch	10^{10} PFU + cisplatin	2	SD
13	Male	62	Squamous	Left mainstem bronchus	Chemotherapy; radiotherapy	cT4N3M0 stage IIIB	Bronch	10^{11} PFU	1	Not assessable†
14	Male	70	Squamous	Left upper lobe	Chemotherapy	cT2N2M0 stage IIIA	Bronch	10^{11} PFU	4	SD
15	Male	62	Squamous	Right upper lobe	Chemotherapy; radiotherapy	cT4N2M0 stage IIIB	Bronch	10^{11} PFU	4	SD

Abbreviations: Squamous, squamous cell carcinoma; Bronch, bronchoscopic injection; PFU, plaque-forming units; PR, partial response, CT, computed tomography (CT)-guided injection; SD, stable disease; Laser, laser therapy; Adeno, adenocarcinoma.
*Introgen Therapeutics Inc, Houston, TX.
†Tumor sizes could not be measured due to obstructive pneumonia.

months). Two patients (13.3%) were not assessable because their tumor sizes could not be measured due to obstructive pneumonia. Of 13 assessable patients, three patients assessed as having partial response or SD received more than six cycles of ADVEXIN injection alone (patients 1 and 2) or in combination with cisplatin (patient 4) before disease progression. Symptomatic improvement, including reduction in dyspnea, cough, or hemoptysis was observed in four patients (26.7%) with refractory disease. One patient (patient 10) received additional external radiation therapy to 60 Gy over 6 weeks after two intratumoral injections of ADVEXIN and systemic administration of cisplatin, and survived for 3.9 months with evidence of the tumor in the right upper lobe. Overall survival analysis by Kaplan and Meier is 40% at 1 year, 13% at 2 years, and 7% at 3 years (Fig 1).

The first responding patient (patient 1) was a 58-year-old male with locally advanced squamous cell carcinoma at the tracheal bifurcation. He was unable to undergo surgery because of poor pulmonary function and received standard chemoradiotherapy. At the time of enrollment, he had relapsed endobronchial tumor in the area from the carina to the left mainstem bronchus, and received ADVEXIN at the 10^9 PFU dose level every 28 days. Four courses of bronchoscopic injection of ADVEXIN at the 10^9 PFU dose level every 4 weeks resulted in a marked tumor regression (Fig 2A) and relief of his symptoms such as hemoptysis, cough, and dyspnea. Pathologic examination demonstrated squamous metaplasia in most lesions, although there was a microscopic residual tumor in the left mainstem bronchus. He received a total of 14 courses of treatment, during which time no tumor progression was noted for approximately 11 months. His treatment was finally discontinued because of additonal local tumor progression.

The second responding patient (patient 2) presented with locally advanced unresectable squamous cell carcinoma that was completely obstructing the left lower lobe. After two courses of broncoscopic ADVEXIN injection at 10^9 PFU, radiographic tumor destruction was observed at the central portion (Fig 2B), resulting in reopening of the airway. He showed a significant improvement in breathing; treatment was, however, discontinued after nine courses of injections when distant bone metastasis was diagnosed.

A long-term SD was documented in a 46-year-old female with adenocarcinoma at the left upper lobe with multiple intrapulmonary metastasis (patient 4). She had disease progression during chemotherapy using cisplatin, vincristine, and etoposide as noted by a radiographic increase during the preceding 3 months, and received CT-guided injection of ADVEXIN at 10^9 PFU after systemic administration of cisplatin at 80 mg/m^2 every 28 days. Her primary adenocarcinoma in the left upper lobe as well as multiple pulmonary metastases were stable for approximately 10 months during the period of treatment (Fig 2C).

Immune Response to Adenovirus and p53

Fourteen of 15 patients (93.3%) were tested at baseline for neutralizing antibody to Ad5. Six of these patients showed low ($\leq$ 1:20) neutralizing antibody titers, and the other eight patients had titers ranging from 1:20 to 1:320. Titers of specimens collected at 4 weeks after the first injection of ADVEXIN were higher than the titers at baseline in 13 of 14 (92.9%) assessable patients, although the magnitude of increase in titer varied (Table 3). There was a correlation between the dose of the vector and the fold increase in the antibody

Table 2. Adverse Events Observed in Patients Who Received Injections of ADVEXIN™ Summary by Toxicity Grade

Toxicity	ADVEXIN Alone (n = 9) Grade 1	2	3	ADVEXIN + Cisplatin (n = 6) Grade 1	2	3	Total (N = 15) No.	%
Fever	1	7	1	0	5	0	14	93.3
Hemoptysis	6	1	0	2	0	0	9	60.0
Nausea	0	0	0	2	3	0	5	33.3
Vomiting	0	0	0	3	2	0	5	33.3
Cough	3	0	0	1	0	0	4	26.7
Diarrhea	2	0	0	2	0	0	4	26.7
Obstructive pneumonia	0	3	1	0	0	0	4	26.7
Constipation	2	0	0	1	0	0	3	20.0
Back pain	1	1	0	1	0	0	3	20.0
Chest pain	2	0	0	1	0	0	3	20.0
Anemia	0	1	0	0	0	2	3	20.0
Stomatitis	0	0	0	2	0	0	2	13.3
Shoulder pain	0	0	0	2	0	0	2	13.3
Infection	1	1	0	0	0	0	2	13.3
Fatigue	1	0	0	1	0	0	2	13.3
Lumbago	2	0	0	0	0	0	2	13.3
Paracusis	0	0	0	0	2	0	2	13.3
Dyspnea	0	0	1	0	0	0	1	6.7
Pneumonia	0	1	0	0	0	0	1	6.7
Atelectasis	0	0	1	0	0	0	1	6.7
Abdominal fullness	1	0	0	0	0	0	1	6.7
Dysesthesia	0	0	0	1	0	0	1	6.7
Pneumothorax	0	0	0	1	0	0	1	6.7
Hematoma	0	0	0	1	0	0	1	6.7
Pituita	0	0	0	1	0	0	1	6.7
Pleural effusion	1	0	0	0	0	0	1	6.7
Anal bleeding	1	0	0	0	0	0	1	6.7
Tooth pain	1	0	0	0	0	0	1	6.7
Bronchitis	0	0	0	0	1	0	1	6.7
Dysthymia	0	0	0	1	0	0	1	6.7
Injection site pain	0	0	0	1	0	0	1	6.7
Leukopenia	1	0	0	0	0	0	1	6.7
Anorexia	0	1	0	0	0	0	1	6.7
Weight loss	0	0	0	0	0	1	1	6.7
Finger abscess	0	0	0	1	0	0	1	6.7
Arm pain	0	0	0	0	1	0	1	6.7

NOTE. Toxicity defined by National Cancer Institute Common Toxicity Criteria (grade 1 to 4).
*Introgen Therapeutics Inc, Houston, TX.

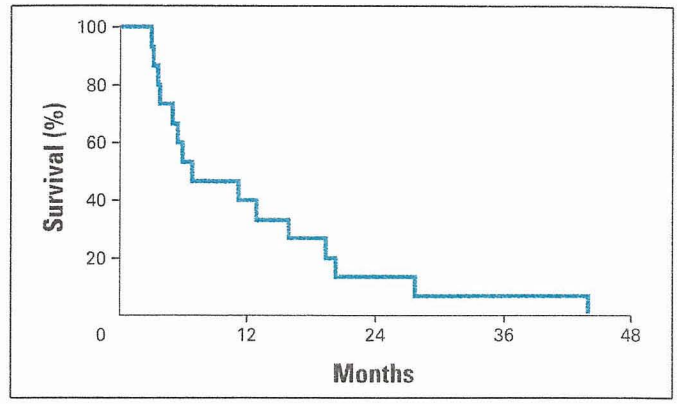

Fig 1. Kaplan-Meier analysis for overall survival of patients studied.

titer (average/median fold increase in titer for 10^9; 10^{10}; 10^{11} PFU doses were: 27; 432; 516/16; 256; 516). Neutralizing antibody titers remained elevated in all patients assessed throughout the study. Two of 13 patients tested (patients 7 and 11) had detectable anti-p53 antibody levels at baseline. Anti-p53 titers increased after six courses and the first course of ADVEXIN administration in patients 2 and 4, respectively. The other nine patients remained negative for anti-p53 antibodies throughout the treatment.

Vector Shedding and Biodistribution

A total of 624 gargle and urine samples from 12 patients were examined for virus shedding by DNA-PCR using vector-specific primers (Table 4, Fig 2). Samples were collected just before vector injection and daily thereafter for 15 days in each course. Vector DNA was detectable in 29 of 39 (74.4%) gargle samples obtained at day 1 after vector injection, regardless of dose level or treatment course, and declined to undetectable levels within 15 days for most patients. One patient (patient 11) was continuously positive for vector DNA until day 15 or beyond, probably due to the shedding of infected tumor cells. In total, 90 gargle samples (14.4%) were positive for vector DNA, whereas vector was detected in only 13 urine specimens (2.1%). The presence of ADVEXIN was assayed in the plasma obtained before and 30, 60, 90 minutes after vector injection (Fig 3). In all 12 patients tested, vector was detected in plasma 30 minutes after injection either by the DNA-PCR or CPE method, and the titers decreased over the next 60 minutes. No correlation was noted between systemic virus titer and AEs or clinical response.

Pathologic and Molecular Analysis of Tumor Biopsy Tissues

Tumor biopsy samples obtained before and 48 hours after vector injection in 12 patients were assessed for *p53* mRNA expression by RT-PCR analysis using vector-specific primers (Table 5). All pretreatment samples were negative for *p53* transgene expression because the primers can distinguish exogenous wt-*p53* from pre-existing mutant *p53* in tumor specimens. Vector-specific *p53* mRNA expression was detectable in 9 of 12 patients (75%) after the first vector injection. Overall, 11 of 12 patients (91.7%) demonstrated positive *p53* transgene expression during the treatment. Of note, *p53* mRNA expression was consistently positive in 52 of 57 serial postinjection samples (91.2%) obtained from patients who received more than six courses of injection (patients 1, 2, and 4). To evaluate the biologic activity of ADVEXIN-induced *p53* expression, we performed quantitative analysis of *p53*-targeted gene expression by a real-time RT-PCR method. Paired biopsy samples obtained before and 48 hours after injection at courses 1, 5, 8, and 11 were analyzed in patient 1 for expression of exogenous *p53*, *p21*, *Noxa*, and *p53AIP1* mRNAs. We found that apoptosis-related gene expression such as *Noxa* and *p53AIP1* was consistently higher in postinjection samples than that in preinjection biopsies throughout the study (Fig 4). The expression patterns of these mRNAs almost paralleled that of exogenous *p53*. In contrast, *p21* expression pattern varied on courses.

Autopsy results were obtained from two patients (patients 3 and 7) who died 25 and 151 days after receiving their fourth and second injection of the vector, respectively. DNA-PCR assay indicated that ADVEXIN was present in tumor tissue as well as proximal lymph nodes, suggesting regional spread of the vector via the lymphatic

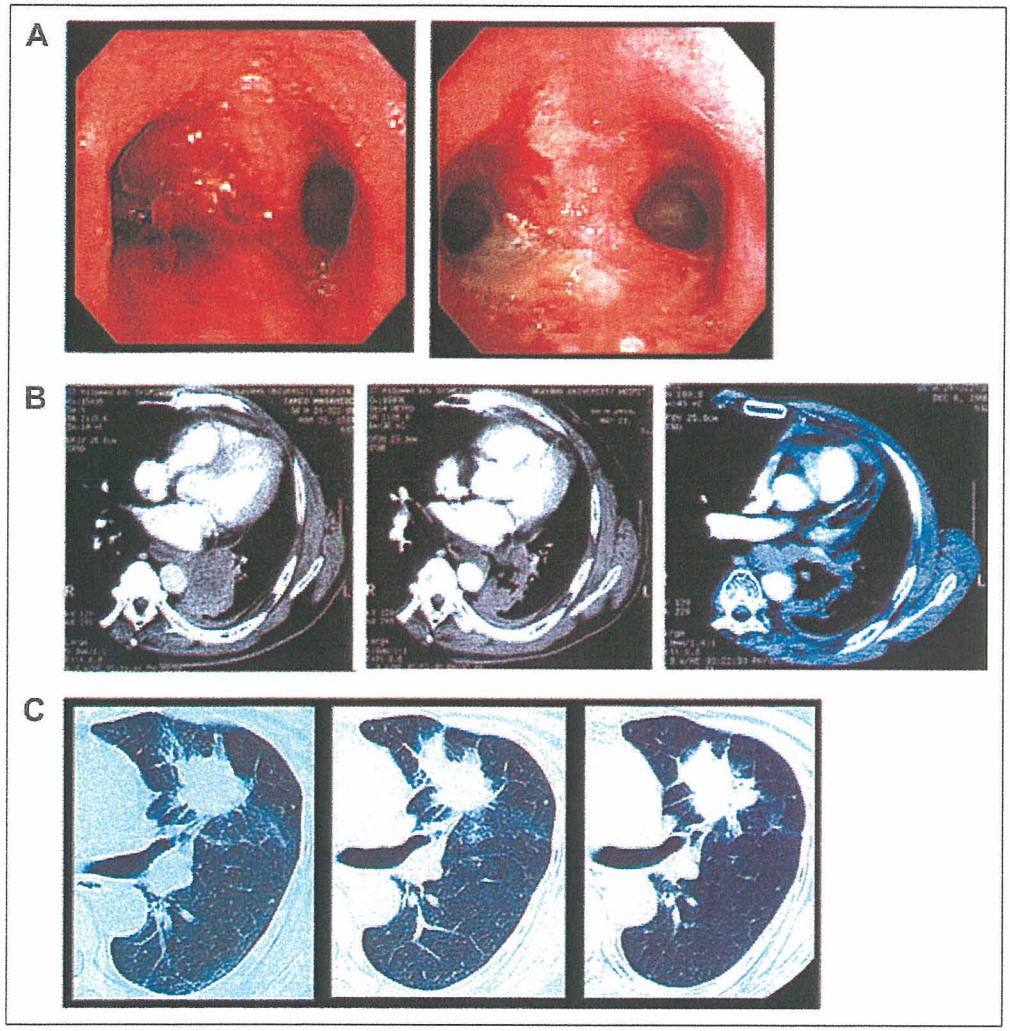

Fig 2. (A) Patient 1 bronchoscopic appearance at the time of enrollment (left) and after four cycles of injections (right). (B) Patient 2 computed tomography scans at baseline (left), at month 2 (middle), and at month 9 (right). (C) Patient 4 computed tomography scans at baseline (left), after four cycles (middle), and 10 cycles (right).

vessels. In contrast, viral distribution was not detected in other organs including liver, kidney, testis, and distal lymph nodes.

DISCUSSION

In an effort to determine the feasibility of *p53* gene therapy in human cancer treatments, several clinical trials of locoregional administration of adenoviral *p53* have been conducted in patients with a variety of advanced malignancies such as NSCLC,[18-20,22] head and neck cancer,[23] bladder cancer,[24,25] recurrent glioma,[26] and ovarian cancer.[27] No available data, however, has been reported yet evaluating this agent in Japanese patients. As clinical trials of the epidermal growth factor receptor tyrosine kinase inhibitor, gefitinib (Iressa; AstraZeneca, London, United Kingdom), revealed significant variability in the response to this drug, with higher responses seen in Japanese patients than in a predominantly European-derived population,[28] it is important to evaluate variations in the response and safety profiles of novel therapeutic agents in Japanese patients. The results of the present multicenter phase I trial indicate that intratumoral administration of ADVEXIN is feasible, safe, and well tolerated in Japanese patients.

Fever was observed as the most common treatment-related AE, which could be due to the transient systemic spread of the vector itself. In fact, flu-like symptoms, such as chills, fatigue or lethargy, and diarrhea, frequently occurred in patients who received replication-competent adenovirus[29,30]; these symptoms, however, are rarely seen in patients treated with ADVEXIN. Although the frequency of fever (affecting 93.3% of the patients) was slightly higher in our trial than those in the United States (79%) or European (76%) trials,[20,22] the observation that most episodes recovered within 48 hours after injection suggests that ADVEXIN-related AEs are limited, and only mild to moderate in severity.

The vector was shed into gargle specimens especially when bronchoscopically injected as expected, whereas vector was rarely detectable in urine despite of the systemic spread of the vector. Most PCR-positive gargle samples were negative by CPE assay (data not shown), indicating that secondary infection through vector shedding into gargle is unlikely to occur. The observation of systemic dissemination of ADVEXIN, which was maximal at 30 minutes after injection, is consistent with that observed in the United States trial, although the highest vector titer in the plasma was approximately $\log_1$ to $\log_2$ lower in Japanese patients.[21] The organ distribution of virus found in two deceased patients is clearly of interest, because, to the best of our knowledge, this is the first evidence of virus spread in the regional lymphatic tissues in humans. It has been reported that replication-deficient adenovirus expressing the *lacZ* gene could be

Table 3. Titers of Neutralizing Anti-Ad5 Antibody and Anti-p53 Antibody After ADVEXIN® Injections

Patient No.	Viral Dose ± Cisplatin	Antibody Titer or Positivity†						
		Baseline	Course 2	Course 3	Course 4	Course 5	Course 6	Course 7
Neutralizing anti-Ad5 antibody								
1	10^9 PFU	1:20	1:1,280	1:1,280	1:2,560	1:1,280	1:1,280	1:2,560
2	10^9 PFU	< 1:20	1:320	1:320	1:640	1:320	1:160	1:160
3	10^9 PFU	< 1:20	1:20	1:40	1:20	NA	NA	NA
4	10^9 PFU + cisplatin	1:320	1:160	1:1,280	1:1,280	1:1,280	1:1,280	1:5,120
5	10^9 PFU + cisplatin	1:40	> 1:20,480	1:2,560	NA	NA	NA	NA
6	10^9 PFU + cisplatin	< 1:20	1:2,560	NA	NA	NA	NA	NA
7	10^{10} PFU	1:20	1:20,480	NA	NA	NA	NA	NA
8	10^{10} PFU	1:20	1:5,120	NA	NA	NA	NA	NA
9	10^{10} PFU	1:320	1:5,120	1:10,240	1:10,240	NA	NA	NA
10	10^{10} PFU + cisplatin	1:40	> 1:20,480	NA	NA	NA	NA	NA
11	10^{10} PFU + cisplatin	< 1:20	1:80	1:5,120	NA	NA	NA	NA
12	10^{10} PFU + cisplatin	< 1:20	1:160	1:2,560	1:1,280	NA	NA	NA
13	10^{11} PFU	NA	NA	NA	NA	NA	NA	NA
14	10^{11} PFU	1:64	1:2,048	1:1,024	1:2,048	NA	NA	NA
15	10^{11} PFU	< 4	> 1:4,096	> 1:4,096	> 1:4,096	NA	NA	NA
Anti-p53 antibody								
1	10^9 PFU	–	–	–	–	–	–	–
2	10^9 PFU	–	–	–	–	–	–	+
3	10^9 PFU	–	–	–	–	NA	NA	NA
4	10^9 PFU + cisplatin	–	+	+	+	–	+	+
5	10^9 PFU + cisplatin	NA	NA	–	NA	NA	NA	NA
6	10^9 PFU + cisplatin	–	–	NA	NA	NA	NA	NA
7	10^{10} PFU	+	+	NA	NA	NA	NA	NA
8	10^{10} PFU	–	–	NA	NA	NA	NA	NA
9	10^{10} PFU	–	–	–	–	NA	NA	NA
10	10^{10} PFU + cisplatin	–	–	NA	NA	NA	NA	NA
11	10^{10} PFU + cisplatin	+	+	+	NA	NA	NA	NA
12	10^{10} PFU + cisplatin	–	–	–	–	NA	NA	NA
13	10^{11} PFU	NA	NA	NA	NA	NA	NA	NA
14	10^{11} PFU	–	–	–	–	NA	NA	NA
15	10^{11} PFU	NA	NA	NA	NA	NA	NA	NA

Abbreviations: PFU, plaque-forming units; NA, not available.
*Introgen Therapeutics Inc, Houston, TX.
†Samples were collected before each course of treatment.

transferred into regional lymph nodes of the stomach in dogs after intratumoral injection[31]; no lymph node tissues, however, were analyzed in any published clinical trials. This finding suggests that intratumorally administered ADVEXIN can spread not only into the blood circulation, but also into the lymphatic vessels, and potentially kill metastatic tumor cells in regional lymph nodes. Schuler et al[22] have reported that intratumoral adenoviral *p53* gene therapy provides no additional benefit in NSCLC patients receiving systemic chemotherapy by comparing the responses of injected lesions with those of noninjected comparator lesions, such as hilar metastatic tumors. According to our biodistribution data, the possibility that their virus spread into comparator lesions and showed antitumor effect cannot be ruled out.

Despite the presence of neutralizing antibodies for adenovirus, we found that *p53* transgene expression was detected in most patients throughout the period of treatment. In addition, quantitative real-time RT-PCR analysis demonstrated that the expression patterns of apoptosis-related *p53*-targeted genes such as *Noxa* and *p53AIP1* paralleled that of exogenous *p53* (Fig 4), demonstrating that exogenous *p53* produced after ADVEXIN treatment has biologic activity. These findings further demonstrate that circulating neutralizing anti-Ad5 antibodies do not inhibit vector-mediated transgene expression when ADVEXIN is directly injected into the tumors. Two of 13 patients (15.4%) had pre-existing anti-p53 antibodies, which is consistent with previous studies reporting that p53 autoantibodies were detected in 10% to 20% of patients with lung cancer.[32] Most patients, however, did not exhibit an increase of anti-p53 titers after ADVEXIN injection, presumably because of the short half-life of wt-p53 protein or due to lack of overcoming tolerance to this self protein.

As predicted by our preclinical and other clinical studies,[10-20] sustained antitumor effect was seen with tumor regression or stabilization of tumor growth in 11 of 13 assessable patients. Patient 1 exhibited a 50% or greater reduction in tumor size after ADVEXIN injection and this response was maintained with monthly injections; the growth rate of tumor, however, suddenly increased at 11 months after the time of entry, leading to the uncontrollable progressive disease. Although the molecular mechanism of this resistance to treatment is still under investigation, increasing the frequency of administration beyond once per month may be an approach to improve efficacy in such patients. Previous experience with ADVEXIN has shown that patients with airway stenosis or obstruction may be suitable candidates for this locoregional therapy.[18-20] Indeed, three patients (patients 1, 2, and 15) exhibited significant reopening of

Table 4. Vector Shedding Into Gargle and Urine After ADVEXIN® Injections

Course of Viral Dose ± Cisplatin	DNA-PCR Results: Gargle (day)															
	Pre	1	2	3	4	5	6	7	8	9	10	11	12	13	14	15
10^9 PFU (patient 1)																
1	−	+	+	−	+	−	−	−	−	−	−	−	−	−	−	−
2	−	−	+	+	−	−	−	−	−	−	−	−	−	−	−	−
3	−	−	−	−	−	−	−	−	−	+	−	−	−	−	−	−
4	+	+	−	−	−	−	−	−	−	−	−	−	−	−	−	−
5	−	+	−	−	+	−	−	−	−	−	−	−	−	−	−	−
6	−	+	−	−	−	−	−	−	−	−	−	−	−	−	−	−
10^9 PFU (patient 2)																
1	−	+	+	+	−	−	−	−	−	−	−	−	−	−	−	−
2	−	+	+	−	+	−	−	−	−	−	−	−	−	−	−	−
3	−	+	+	+	−	−	−	−	−	−	−	−	−	−	−	−
4	−	+	−	−	+	−	−	+	−	−	−	−	+	−	−	−
5	−	+	+	+	−	−	−	−	−	−	+	−	−	−	−	−
6	−	+	−	−	+	−	+	−	−	+	−	+	−	−	−	−
10^9 PFU (patient 3)																
1	−	−	−	−	−	−	−	−	−	−	−	−	−	−	−	−
2	−	+	−	−	−	−	−	−	−	−	−	−	−	−	−	−
3	−	+	−	−	−	−	−	−	−	−	−	−	−	−	−	−
4	−	+	−	−	−	−	−	−	−	−	−	−	−	−	−	−
10^9 PFU + cisplatin (patient 4)																
1	−	−	−	−	−	−	−	−	−	−	−	−	−	−	−	−
2	−	−	−	−	−	−	−	−	−	−	−	−	−	−	−	−
3	−	−	−	−	−	−	−	−	−	−	−	−	−	−	−	−
4	−	+	−	+	−	−	−	−	−	−	−	−	−	−	−	−
5	−	−	−	−	−	−	−	−	−	−	−	−	−	−	−	−
6	−	+	−	−	−	−	−	−	−	−	−	−	−	−	−	−
10^9 PFU + cisplatin (patient 5)																
1	−	+	+	−	−	−	−	−	−	−	−	−	−	−	−	−
2	−	−	−	−	−	−	−	−	−	−	−	−	−	−	−	−
3	−	+	+	−	−	−	−	−	−	−	−	−	−	−	−	−
10^9 PFU + cisplatin (patient 6)																
1	−	−	−	−	−	−	−	−	−	−	−	−	−	−	−	−
2	−	−	−	−	−	−	−	−	−	−	−	−	−	−	−	−
10^{10} PFU (patient 7)																
1	−	+	+	+	−	+	−	−	−	−	−	−	−	−	−	−
2	−	+	+	−	−	−	−	−	−	−	−	−	−	−	−	−
10^{10} PFU (patient 8)																
1	−	+	−	−	−	+	−	+	+	−	−	−	−	+	−	−
10^{10} PFU (patient 9)																
1	−	+	+	−	−	−	−	−	−	−	−	−	−	−	−	−
2	−	+	+	−	−	−	−	−	−	−	−	−	−	−	−	−
3	−	+	−	−	−	+	−	−	−	−	−	−	−	−	−	−
4	−	+	−	−	−	−	−	−	−	−	−	−	−	−	−	−
10^{10} PFU + cisplatin (patient 10)																
1	−	+	−	−	+	−	−	−	−	−	−	−	−	−	−	−
10^{10} PFU + cisplatin (patient 11)																
1	−	+	−	+	−	−	−	−	+	−	−	−	+	−	−	−
2	−	+	+	+	+	+	+	+	+	+	+	+	+	+	+	+
10^{10} PFU + cisplatin (patient 12)																
1	−	+	+	−	+	−	+	−	−	−	−	−	−	−	−	−
2	−	+	+	−	+	+	−	−	−	−	−	−	−	−	−	−
10^9 PFU (patient 1)																
1	−	−	−	−	−	−	−	−	−	−	−	−	−	−	−	−
2	−	−	−	−	−	−	−	−	−	−	−	−	−	−	−	−
3	−	−	−	−	−	−	−	−	−	−	−	−	−	−	−	−
4	−	−	−	−	−	−	−	−	−	−	−	−	−	−	−	−
5	−	−	−	−	−	−	−	−	−	−	−	−	−	−	−	−
6	−	−	−	−	−	−	−	−	−	−	−	−	−	−	−	−

(continued on following page)

Table 4. Vector Shedding Into Gargle and Urine After ADVEXIN™ Injections (continued)

Course of Viral Dose ± Cisplatin	DNA-PCR Results															
	Urine (day)															
	Pre	1	2	3	4	5	6	7	8	9	10	11	12	13	14	15
10^9 PFU (patient 2)																
1	–	–	–	–	–	–	–	–	–	–	–	–	–	–	–	–
2	–	–	–	–	–	–	–	–	–	–	–	–	–	–	–	–
3	–	–	–	–	–	–	–	–	–	–	–	–	–	–	–	–
4	–	–	–	–	–	–	–	–	–	–	–	–	–	–	–	–
5	–	–	–	–	–	–	–	–	–	–	–	–	–	–	–	–
6	–	–	–	–	–	–	–	–	–	–	–	–	–	–	–	–
10^9 PFU (patient 3)																
1	–	–	–	–	–	–	–	–	–	–	–	–	–	–	–	–
2	–	–	–	–	–	–	–	–	–	–	–	–	–	–	–	–
3	–	–	–	–	–	–	–	–	–	–	–	–	–	–	–	–
4	–	–	–	–	–	–	–	–	–	–	–	–	–	–	–	–
10^9 PFU + cisplatin (patient 4)																
1	–	–	–	–	–	–	–	–	–	–	–	–	–	–	–	–
2	–	–	–	–	–	–	–	–	–	–	–	–	–	–	–	–
3	–	–	–	–	–	–	–	–	–	–	–	–	–	–	–	–
4	–	–	–	–	–	–	–	–	–	–	–	–	–	–	–	–
5	–	–	–	–	–	–	–	–	–	–	–	–	–	–	–	–
6	–	–	–	–	–	–	–	–	–	–	–	–	–	–	–	–
10^9 PFU + cisplatin (patient 5)																
1	–	–	–	–	–	–	–	–	–	–	–	–	–	–	–	–
2	–	–	–	–	–	–	–	–	–	–	–	–	–	–	–	–
3	–	–	–	–	–	–	–	–	–	–	–	–	–	–	–	–
10^9 PFU + cisplatin (patient 6)																
1	–	–	–	–	–	–	–	–	–	–	–	–	–	–	–	–
2	–	–	–	–	–	–	–	–	–	–	–	–	–	–	–	–
10^{10} PFU (patient 7)																
1	–	–	–	–	–	–	–	–	–	–	–	–	–	+	–	–
2	–	–	–	–	–	–	–	–	–	+	–	+	+	+	+	–
10^{10} PFU (patient 8)																
1	–	–	–	–	–	–	–	–	–	–	–	–	–	–	–	–
10^{10} PFU (patient 9)																
1	–	–	–	–	–	–	–	–	–	–	–	–	–	–	–	–
2	–	–	–	+	+	+	+	+	–	–	+	–	–	–	–	–
3	–	–	–	–	–	–	–	–	–	–	–	–	–	–	–	–
4	–	–	–	–	–	–	–	–	–	–	–	–	–	–	–	–
10^{10} PFU − cisplatin (patient 10)																
1	–	–	–	–	–	–	–	–	–	–	–	–	–	–	–	–
10^{10} PFU + cisplatin (patient 11)																
1	–	–	–	–	–	+	–	–	–	–	–	–	–	–	–	–
2	–	–	–	–	–	–	–	–	–	–	–	–	–	–	–	–
10^{10} PFU + cisplatin (patient 12)																
1	–	–	–	–	–	–	–	–	–	–	–	–	–	–	–	–
2	–	–	–	–	–	–	–	–	–	–	–	–	–	–	–	–

Abbreviations: PCR, polymerase chain reaction; PFU, plaque-forming units.
[†]Introgen Therapeutics Inc, Houston, TX.

the airway after bronchoscopic injection of ADVEXIN, and resulted in the marked improvement of symptoms such as cough, hemoptysis, and dyspnea.

It is of interest that three of six patients who were assigned to the cohort with the lowest dose of ADVEXIN could receive more than six courses of treatment, whereas no patients treated with higher doses completed six cycles of injections. There was a possible selection bias of patients related to the dose levels and the centers; this finding, however, suggests that 10^9 PFU of ADVEXIN appears to be sufficient to induce local effect without toxicities in certain patients. Another surprising observation from this study is that there was no apparent difference in clinical activity between the groups with ADVEXIN alone and ADVEXIN plus cisplatin. One possible explanation for this result is that cisplatin may affect induction of systemic immune response against mutant-p53–expressing tumor cells triggered by ADVEXIN. Support for this hypothesis is found in the reduced levels of anti-Ad5 antibodies in the high-dose ADVEXIN plus cisplatin group compared with high-dose

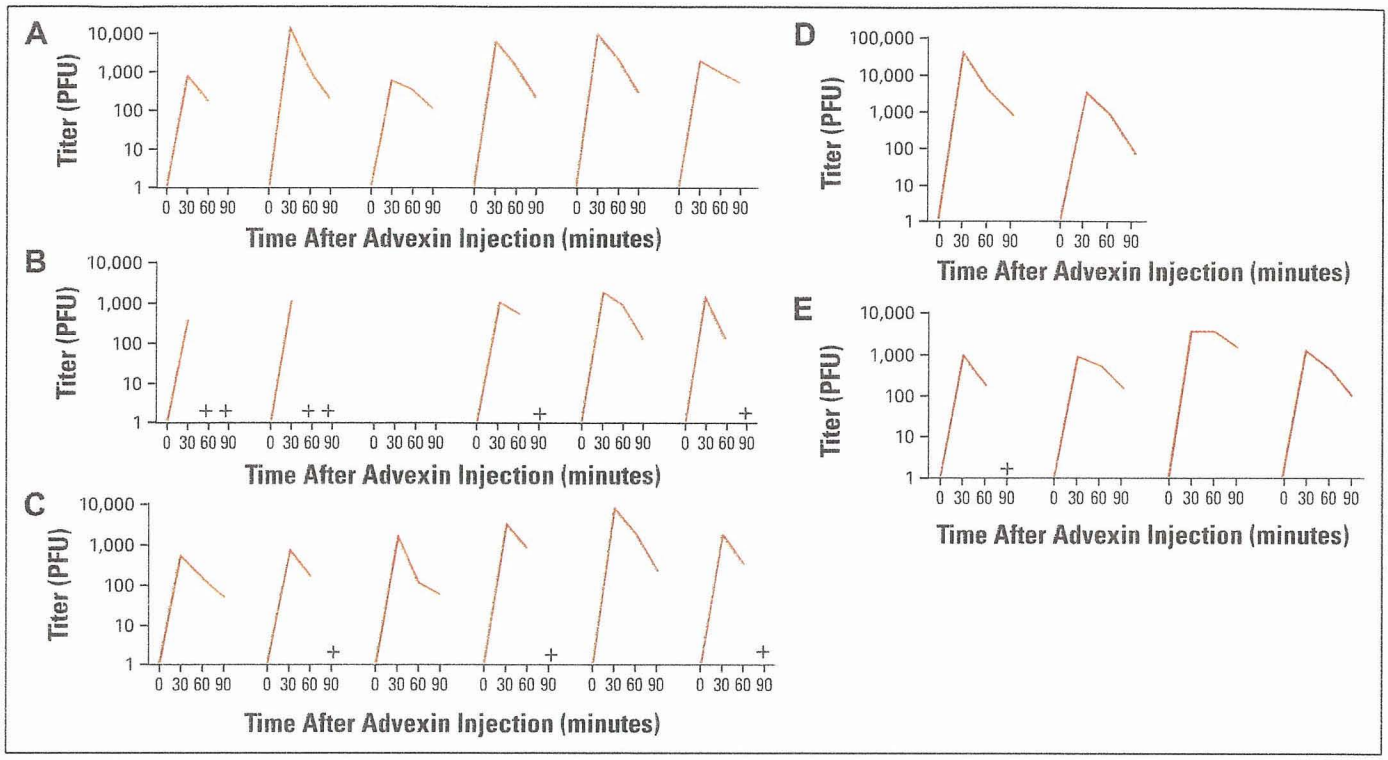

Fig 3. Quantitative detection of ADVEXIN (Introgen, Houston, TX) the cytopathic effect (CPE) assay in the plasma obtained before and 30, 60, and 90 minutes after vector injection. (A) Patient 1; (B) patient 2; (C) patient 4; (D) patient 7; and (E) patient 9. (−) Indicates negative by the CPE assay, but positive by a DNA-polymerase chain reaction analysis.

ADVEXIN as monotherapy. Furthermore, the study was not powered to identify differences in these groups.

In conclusion, this study demonstrates that repeated intratumoral injections of ADVEXIN in combination with or without cisplatin are feasible and well tolerated in Japanese patients. Despite undergoing more treatment cycles than other trials, patients experienced no severe toxicities and exhibited a long-term clinical activity (≥ 9 months in 20% of patients). Therefore, it seems to be reasonable to explore the antitumor effect of this virus in patients with earlier-stage disease. This study provides support for the ongoing randomized phase III trials to identify the therapeutic benefit of ADVEXIN in squamous cell carcinoma of the head and neck and suggest that additional evaluations for NSCLC in phase II/III trials with appropriate controls are warranted.

Table 5. Vector-Specific *p53* mRNA Expression in Tumor Tissues After ADVEXIN* Injections

Patient No.	Viral Dose ± Cisplatin	RT-PCR Results Course 1	Course 2	Course 3	Course 4	Course 5	Course 6	Course 7	Course 8	Course 9	Course 10	Course 11	Course 12	Course 13	Course 14
1	10^{9} PFU	−/+	±	+/+	±	+/+	+/+	+/+	−/+	−/+	+/+	+/+	±	+/+	+/NA
2	10^{9} PFU	−/+	+/+	+/+	+/+	+/+	+/+	+/+	+/+	+/NA					
3	10^{9} PFU	−/−	−/−	+/+	+/+										
4	10^{9} PFU + cisplatin	−/+	+/+	+/+	+/+	+/+	+/+	+/+	+/+	+/NA					
5	10^{9} PFU + cisplatin	−/+	+/+	+/+											
6	10^{9} PFU + cisplatin	−/−	−/−												
7	10^{10} PFU	−/−	−/−	+/NA											
8	10^{10} PFU	−/+	−/NA												
9	10^{10} PFU	−/+	−/+	±	+/+										
10	10^{10} PFU + cisplatin	−/+													
11	10^{10} PFU + cisplatin	−/+	+/+	+/ NA											
12	10^{10} PFU + cisplatin	−/+	+/+	−/−	−/NA										

NOTE. Paired samples were collected before and 48 hours after AVEXIN injection in each course of treatment.
Abbreviations: PFU, plaque-forming units; NA, not available.
*Introgen Therapeutics Inc, Houston, TX.

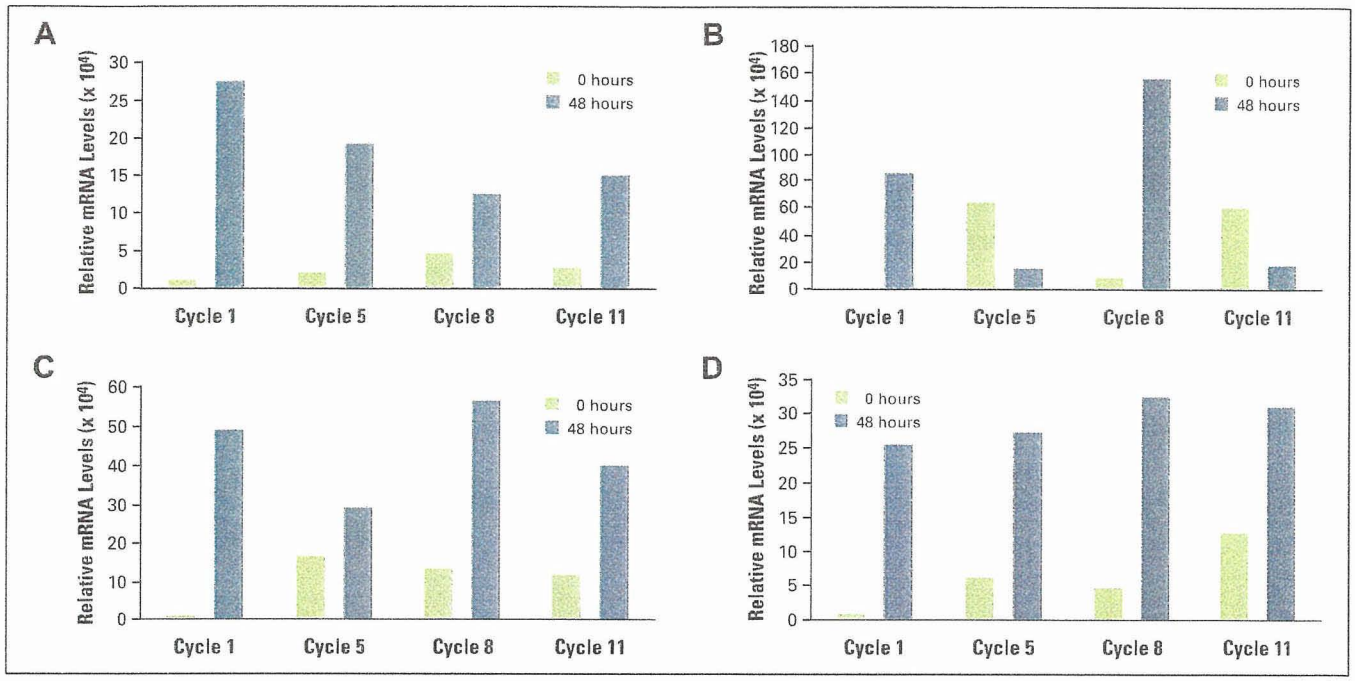

Fig 4. Expression of exogenous *p53* mRNA and *p53*-targeted gene mRNAs (*p21, Noxa*, and *p53AIP1*) was measured by the real-time quantitative polymerase chain reaction assay. (A) *p53*, (B) *p21*, (C) *Noxa*, and (D) *p53AIP1*. Tumor biopsy samples were obtained before and 48 hours after ADVEXIN (Introgen Therapeutics Inc, Houston, TX) injection at the indicated cycle (one, three, eight, and 11) in patient 1. All expression levels are normalized to that of β-Globin.

REFERENCES

1. Greenlee RT, Murray T, Bolden S, et al: Cancer statistics, 2000. CA Cancer J Clin 50:7-33, 2000
2. Statistics and Information Department, Minister's Secretariat, Ministry of Health and Welfare. Vital Statistics 2001 Japan. Tokyo, Japan, Health and Welfare Statistics Association, 2003
3. Minna JD, Roth JA, Gazdar AF: Focus on lung cancer. Cancer Cell 1:49-52, 2002
4. Hollstein M, Sidransky D, Vogelstein B, et al: p53 mutations in human cancers. Science 253:49-53, 1991
5. Greenblatt MS, Bennett WP, Hollstein M, et al: Mutations in the p53 tumor suppressor gene: Clues to cancer etiology and molecular pathogenesis. Cancer Res 54:4855-4878, 1994
6. Horio Y, Takahashi T, Kuroishi T, et al: Prognostic significance of p53 mutations and 3p deletions in primary resected non-small cell lung cancer. Cancer Res 53:1-4, 1993
7. Nishio M, Koshikawa T, Kuroishi T, et al: Prognostic significance of abnormal p53 accumulation in primary, resected non–small-cell lung cancers. J Clin Oncol 14:497-502, 1996
8. Levine AJ: p53, the cellular gatekeeper for growth and division. Cell 88:323-331, 1997
9. Fujiwara T, Cai DW, Georges RN, et al: Therapeutic effect of a retroviral wild-type p53 expression vector in an orthotopic lung cancer model. J Natl Cancer Inst 86:1458-1462, 1994
10. Kagawa S, Fujiwara T, Hizuta A, et al: p53 expression overcomes $p21^{WAF1/CIP1}$-mediated G1 arrest and induces apoptosis in human cancer cells. Oncogene 15:1903-1909, 1997
11. Shao J, Fujiwara T, Kadowaki Y, et al: Overexpression of the wild-type p53 gene inhibits NF-κB activity and synergizes with aspirin to induce apoptosis in human colon cancer cells. Oncogene 19:726-736, 2000
12. Tango Y, Taki M, Shirakiya Y, et al: Late resistance to adenoviral p53-mediated apoptosis caused by decreased expression of coxsackie-adenovirus receptors in human lung cancer cells. Cancer Sci 95:459-463, 2004
13. Ohtani S, Kagawa S, Inago Y, et al: Quantitative analysis of p53-targeted gene expression and visualization of p53 transcriptional activity following intratumoral administration of adenoviral p53 in vivo. Mol Cancer Ther 3:93-100, 2004
14. Fujiwara T, Grimm EA, Mukhopadhyay T, et al: Induction of chemosensitivity in human cancer cells in vivo by adenoviral-mediated transfer of the wild-type p53 gene. Cancer Res 54:2287-2291, 1994
15. Ogawa N, Fujiwara T, Kagawa S, et al: Novel combination therapy for human colon cancer with adenovirus-mediated wild-type p53 gene transfer and DNA-damaging chemotherapeutic agent. Int J Cancer 73:367-370, 1997
16. Nishizaki M, Fujiwara T, Tanida T, et al: Recombinant adenovirus expressing wild-type p53 is antiangiogenic: A proposed mechanism for bystander effect. Clin Cancer Res 5:1015-1023, 1999
17. Waku T, Fujiwara T, Shao J, et al: Contribution of CD95 ligand-induced neutrophil infiltration to the bystander effect in p53 gene therapy for human cancer. J Immunol 165:5884-5890, 2000
18. Swisher SG, Roth JA, Nemunaitis J, et al: Adenovirus-mediated p53 gene transfer in advanced non–small-cell lung cancer. J Natl Cancer Inst 91: 763-771, 1999
19. Nemunaitis J, Swisher SG, Timmons T, et al: Adenovirus-mediated p53 gene transfer in sequence with cisplatin to tumors of patients with non–small-cell lung cancer. J Clin Oncol 18:609-622, 2000
20. Swisher SG, Roth JA, Komaki R, et al: Induction of p53-regulated genes and tumor regression in lung cancer patients after intratumoral delivery of adenoviral p53 (INGN 201) and radiation therapy. Clin Cancer Res 9 93-101, 2003
21. Zhang WW, Fang X, Mazur W, et al: High efficiency gene transfer and high-level expression of wildtype p53 in human lung cancer cells mediated by recombinant adenovirus. Cancer Gene Ther 1.5-13, 1994
22. Schuler M, Herrmann R, De Greve JL, et al: Adenovirus-mediated wild-type p53 gene transfer in patients receiving chemotherapy for advanced non-small-cell lung cancer: Results of a multicenter phase II study. J Clin Oncol 19:1750-1758, 2001
23. Clayman GL, el-Naggar AK, Lippman SM, et al: Adenovirus-mediated p53 gene transfer in patients with advanced recurrent head and neck squamous cell carcinoma. J Clin Oncol 16:2221-2232, 1998
24. Kuball J, Wen SF, Leissner J, et al: Successful adenovirus-mediated wild-type p53 gene transfer in patients with bladder cancer by intravesical vector instillation. J Clin Oncol 20:957-965, 2002
25. Pagliaro LC, Keyhani A, Williams D, et al: Repeated intravesical instillations of an adenoviral vector in patients with locally advanced bladder cancer: A phase I study of p53 gene therapy. J Clin Oncol 21:2247-2253, 2003
26. Lang FF, Bruner JM, Fuller GN, et al: Phase I trial of adenovirus-mediated p53 gene therapy for recurrent glioma: Biological and clinical results. J Clin Oncol 21: 2508-2518, 2003
27. Buller RE, Runnebaum IB, Karlan BY, et al: A phase I/II trial of rAd/p53 (SCH 58500) gene replacement in recurrent ovarian cancer. Cancer Gene Ther 9:553-566, 2002
28. Fukuoka M, Yano S, Giaccone G, et al: Multi-institutional randomized phase II trial of gefitinib for previously treated patients with advanced non-small-cell lung cancer (The IDEAL 1 Trial). J Clin Oncol 21:2237-2246, 2003
29. Vasey PA, Shulman LN, Campos S, et al: Phase I trial of intraperitoneal injection of the E1B-55-kd-gene-deleted adenovirus ONYX-015 (dl1520) given on days 1 through 5 every 3 weeks in patients with recurrent/refractory epithelial ovarian cancer. J Clin Oncol 20:1562-1569, 2002

30. Hamid O, Varterasian ML, Wadler S, et al: Phase II trial of intravenous CI-1042 in patients with metastatic colorectal cancer. J Clin Oncol 21:1498-1504, 2003

31. Matsukura N, Hoshino A, Igarashi T, et al: In situ gene transfer and suicide gene therapy of gastric cancer induced by N-ethyl-N'-nitro-N-nitrosoguanidine in dogs. Jpn J Cancer Res 90:1039-1049, 1999

32. Mitsudomi T, Suzuki S, Yatabe Y, et al: Clinical implications of p53 autoantibodies in the sera of patients with non-small-cell lung cancer. J Natl Cancer Inst 90:1563-1568, 1998

Acknowledgment

We thank Masafumi Kataoka, MD, Kazuhiko Kataoka, MD, and Osamu Kawamata, MD, for study support; Yoshiko Shirakiya for technical assistance; and Atsushi Nakamura and Takeo Ozawa for study management and monitoring. More importantly, we thank all patients for their courage and cooperation.

Authors' Disclosures of Potential Conflicts of Interest

Although all authors completed the disclosure declaration, the following author or immediate family members indicated a financial interest. No conflict exists for drugs or devices used in a study if they are not being evaluated as part of the investigation. For a detailed description of the disclosure categories, or for more information about ASCO's conflict of interest policy, please refer to the Author Disclosure Declaration and the Disclosures of Potential Conflicts of Interest section in Information for Contributors.

Authors	Employment	Leadership	Consultant	Stock	Honoraria	Research Funds	Testimony	Other
Sunil Chada	Introgen Therapeutics (N/R)							
Dollar Amount Codes	(A) < $10,000	(B) $10,000-99,999	(C) ≥ $100,000	(N/R) Not Required				

Author Contributions

Conception and design: Toshiyoshi Fujiwara, Noriaki Tanaka, Sunil Chada
Administrative support: Toshiyoshi Fujiwara, Yasuo Saijo, Toshihiro Nukiwa, Kunihiko Yoshimura, Tetsuo Sato, Yoshikatsu Eto, Haruhiko Nakamura, Harubumi Kato
Provision of study materials or patients: Toshiyoshi Fujiwara, Noriaki Tanaka, Susumu Kanazawa, Yasuo Saijo, Toshihiro Nukiwa, Kunihiko Yoshimura, Tetsuo Sato, Yoshikatsu Eto, Haruhiko Nakamura, Harubumi Kato
Collection and assembly of data: Toshiyoshi Fujiwara, Yasuo Saijo, Toshihiro Nukiwa, Kunihiko Yoshimura, Tetsuo Sato, Yoshikatsu Eto, Haruhiko Nakamura, Harubumi Kato
Data analysis and interpretation: Toshiyoshi Fujiwara, Shoichiro Ohtani, Sunil Chada
Manuscript writing: Toshiyoshi Fujiwara, Sunil Chada
Final approval of manuscript: Toshiyoshi Fujiwara, Noriaki Tanaka, Susumu Kanazawa, Yasuo Saijo, Toshihiro Nukiwa, Kunihiko Yoshimura, Tetsuo Sato, Yoshikatsu Eto, Sunil Chada, Haruhiko Nakamura, Harubumi Kato

GLOSSARY

Adenoviral p53: The E1- and E3-deleted, replication-deficient adenovirus vector encoding for the wild-type *p53* tumor suppressor gene.

Apoptosis: Also called programmed cell death, it is a signaling pathway that leads to cellular suicide in an organized manner. Several factors and receptors are specific to the apoptotic pathway. The net result is that cells shrink, develop blebs on their surface, and their DNA undergoes fragmentation.

Bystander effect: The biologically positive response observed in untreated cells when neighboring cells are treated. Because of the bystander effect, the magnitude of the therapeutic response exceeds the effect expected from direct target-cell treatment, illustrating that the treatment not only induces direct cytotoxic effects against the individual target cell but also causes the growth suppression of bystander, untreated cells via other mechanisms.

CPE (cytopathic effect): Viruses can infect target cells and cause cell death, referred to as the CPE. A CPE assay can be used to determine the titer of viral stocks.

Noxa: *Noxa* is a proapoptotic member of the *Bcl-2* family, which contains the *Bcl-2* homology 3 (BH3) region, but lacks other BH domains. *Noxa* functions as an early response gene and a mediator of p53-induced apoptosis. In human cells, Noxa is also designated as PMA-induced protein 1 or APR.

p21: The cyclin-dependent kinase inhibitor p21Cip1 inhibits cell-cycle progression by binding to cyclin/CDK complexes and arresting cells in the G1 phase of the cell cycle.

p53: The normal function of p53 is to act as a transcriptional activator of genes with a p53-binding site and an inhibitor of genes lacking a p53 binding site. Expression of high levels of wild-type p53 is associated with cell cycle arrest and apoptosis. Mutations in p53 are seen in several tumors.

p53AIP1 (p53-regulated, apoptosis-inducing protein 1): *p53AIP1* is a tumor suppressor gene that localizes to the mitochondria and regulates mitochondrial membrane potential.

RT-PCR (reverse-transcriptase polymerase chain reaction): PCR is a method that allows logarithmic amplification of short DNA sequences within a longer, double-stranded DNA molecule. Gene expression can be measured after extraction of total RNA and preparation of cDNA by a reverse-transcription step. Thus, RT-PCR enables the detection of PCR products on a real-time basis, making it a sensitive technique for quantitating changes in gene expression.

Tumor suppressor gene: A gene whose protein product is responsible for antiproliferative signals. The retinoblastoma gene product and the product of the p53 gene are two examples of tumor suppressor genes.

Int. J. Cancer: **119**, 432–440 (2006)

Enhanced antitumor efficacy of telomerase-selective oncolytic adenoviral agent OBP-401 with docetaxel: Preclinical evaluation of chemovirotherapy

Toshiya Fujiwara[1], Shunsuke Kagawa[1,2], Hiroyuki Kishimoto[1], Yoshikatsu Endo[1], Masayoshi Hioki[1], Yoshihiro Ikeda[1], Ryo Sakai[1], Yasuo Urata[3], Noriaki Tanaka[1] and Toshiyoshi Fujiwara[1,2]*

[1]*Division of Surgical Oncology, Department of Surgery, Okayama University Graduate School of Medicine and Dentistry, Okayama, Japan*
[2]*Okayama University Hospital, Center for Gene and Cell Therapy, Okayama, Japan*
[3]*Oncolys Biopharma Inc., Tokyo, Japan*

Oncolytic adenoviruses are being developed as novel anticancer therapeutics and currently undergoing clinical trials. We previously demonstrated that telomerase-specific replication-competent adenovirus (Telomelysin: OBP-301), in which the human telomerase reverse transcriptase (hTERT) promoter regulates viral replication, efficiently killed human tumor cells. We further constructed OBP-401 (Telomelysin-GFP) that expresses the green fluorescent protein (*GFP*) reporter gene under the control of the cytomegalovirus promoter in the E3 region to monitor viral distribution. Here, we examined the feasibility of a single-agent therapy with OBP-401 as well as of combining OBP-401 with chemotherapeutic agents. Infection of OBP-401 alone or followed by the treatment of a chemotherapeutic drug, docetaxel (Taxotere), resulted in a profound *in vitro* cytotoxicity and GFP expression in various human cancer cell lines originating from different organs (lung, colon, esophagus, stomach, liver and prostate), although the magnitude of antitumor effect varied among the cell types. Other chemotherapeutic drugs such as vinorelbine (Navelbine) and SN38 (the potent active metabolite of irinotecan) combined with OBP-401 also inhibited the growth of human cancer cells. Quantitative real-time PCR analysis demonstrated that docetaxel did not affect viral replication. For *in vivo* evaluation, *nu/nu* mice xenografted with H1299 human lung tumor received intratumoral injection of OBP-401 and intraperitoneal administration of docetaxel. Analysis of growth of implanted tumors showed a significant, therapeutic synergism, although OBP-401 alone and docetaxel alone showed modest inhibition of tumor growth. Thus, OBP-401 in combination with docetaxel efficiently enhances the antitumor efficacy both *in vitro* and *in vivo*, and the outcome has important implications for tumor-specific oncolytic chemovirotherapies for human cancers.

Key words: oncolytic adenovirus; combination therapy; docetaxel; GFP

Lack of restricted selectivity for tumor cells is the primary limitation of common cancer therapeutics such as chemotherapy and radiotherapy. To improve the therapeutic index, there is a need for anticancer agents that selectively target only tumor cells and spare normal cells. Telomerase is a ribonucleoprotein complex responsible for the complete replication of chromosomal ends.[1] Many studies have demonstrated the expression of telomerase activity in more than 85% of human cancers,[2] but only in few normal somatic cells.[3] Telomerase activation is considered a critical step in carcinogenesis and its activity is closely correlated with human telomerase reverse transcriptase (hTERT) expression.[4] Replication-selective tumor-specific adenoviruses are being developed as novel anticancer therapies.[5–9] We previously developed an adenovirus vector that drives E1A and E1B genes under the hTERT promoter, namely Telomelysin: OBP-301,[10–12] and showed its selective replication as well as profound cytotoxic activity in a variety of human cancer cells. Although the development of OBP-301 as a monotherapy is currently underway clinically based on promising results of preclinical studies, multimodal strategies to enhance antitumor efficacy *in vivo* is essential for successful clinical outcome. In fact, most of the clinical trials for oncolytic viruses have been conducted in combination with chemotherapy or radiotherapy.[13–16]

Docetaxel is an antineoplastic agent and a member of the taxane family, which are novel antimicrotubule agents that promote the assembly of microtubules from tubulin dimers and stabilization of such microtubules by preventing depolymerization. This stability results in the inhibition of the normal dynamic reorganization of the microtubule network that is essential for vital interphase and mitotic cellular functions. In addition, the taxanes induce abnormal arrays of microtubules throughout the cell cycle and multiple asters of microtubules during mitosis and arrest cells especially in G2 and M phases.[17,18] The effectiveness of any chemotherapy against malignant tumors may be increased by dose intensification; however, such strategy is often associated with the appearance of drug-induced toxicities. Ideally, the strategy for effective treatment should include maximizing the dose enhancement while minimizing systemic toxicity.

In the present study, we hypothesized that combination of oncolytic adenoviral agents (with novel mechanisms of action) with chemotherapeutic agents could minimize the toxic side effects of the latter by reducing the concentrations of anticancer drugs. To test our hypothesis, we used a novel oncolytic adenovirus named OBP-401, which expresses the green fluorescent protein (GFP) reporter gene under the control of the cytomegalovirus promoter in the E3 region to monitor viral distribution by its fluorescence. The therapeutic effects of OBP-401 combined with docetaxel were tested both *in vitro* and *in vivo*. The results showed that the combination therapy of OBP-401 and docetaxel produced additive therapeutic benefits over either individual modality. In addition, docetaxel is considered innocuous for replication of OBP-401 because this agent does not inhibit DNA synthesis.

Material and methods

Cell lines and cell cultures

The human non-small cell lung cancer cell lines H1299 and H226Br, the human colorectal carcinoma cell lines SW620 and DLD-1, the human gastric cancer cell line MKN28, the human esophageal cancer cell lines T.Tn and TE8 and the human prostate cancer cell line LNCaP were propagated in monolayer culture in RPMI 1640 supplemented with 10% fetal calf serum (FCS). The human non-small cell lung cancer cell line A549 was cultured in Dulbecco's modified Eagle's medium (DMEM) containing Nutrient Mixture (Ham's F-12). The transformed embryonic kidney cell line 293 and human hepatic cancer cell line HepG2 were grown in DMEM containing high glucose (4.5 g/l) and supplemented with 10% FCS.

Grant sponsors: Ministry of Education, Science, and Culture, Japan; Ministry of Health and Welfare, Japan.
***Correspondence to:** Center for Gene and Cell Therapy, Okayama University Hospital, 2-5-1 Shikata-cho, Okayama 700-8558, Japan.
Fax: +81-86-235-7884, E-mail: toshi_f@md.okayama-u.ac.jp
Received 2 August 2005; Accepted 14 December 2005
DOI 10.1002/ijc.21846
Published online 13 February 2006 in Wiley InterScience (www.interscience.wiley.com).

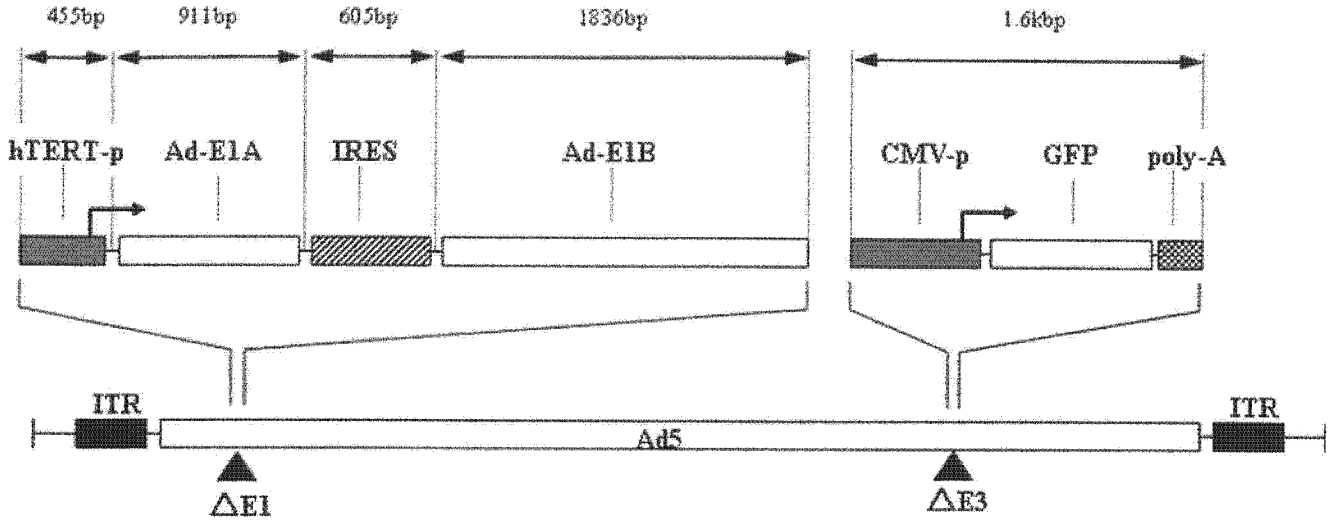

FIGURE 1 – Schematic diagrams of OBP-401DNA structures. OBP-401 is a telomerase-specific replication-competent adenovirus variant, in which the hTERT promoter element drives the expression of E1A and E1B genes linked with an IRES, and GFP gene is inserted under CMV promoter into E3 region for monitoring viral replication.

Chemotherapeutic agents and viruses

Docetaxel (taxotere), SN-38 (topotecin) and vinorelbine (navelbine) were kindly provided by Aventis Pharma (Tokyo, Japan), Daiichi Pharmaceutical Co. (Tokyo) and Kyowa Hakko Kogyo Co. (Tokyo), respectively. These agents were diluted with the respective medium just before use for *in vitro* studies and with phosphate-buffered saline (PBS) for *in vivo* studies. OBP-401 is a telomerase-specific replication-competent adenovirus variant, in which the hTERT promoter element drives the expression of E1A and E1B genes linked with an IRES, with the GFP gene inserted under cytomegalovirus (CMV) promoter into E3 region (Fig. 1). Construction of OBP-401 was described elsewhere. The virus was purified by ultracentrifugation in cesium chloride step gradients, and the titer was determined by plaque assay in 293 cells, as described previously.[19]

Cell viability assay

XTT (sodium 3′-[1-(phenylaminocarbonyl)-3,4-tetrazolium]-bis(4-methoxy-6-nitro) benzene sulfonic acid hydrate) assay was performed by seeding human tumor cells at 1,000 cells/well in 96-well plates 18–20 hr before viral infection. The cells were then infected with OBP-401 at a multiplicity of infection (MOI) of 0.1 and 1 plaque-forming units (PFU)/cell and subsequently treated with chemotherapeutic agents 24 hr after infection. Cell viability was determined at the indicated times by using a Cell Proliferation Kit II (Roche Molecular Biochemicals, Indianapolis, IN) according to the protocol provided by the manufacturer.

Cell killing assay

Human non-small cell lung cancer cell line H1299 and human colorectal carcinoma cell line SW620 were plated on 25-cm^2 flasks at 1×10^5 cells at 48 hr before viral infection. Cells were then infected with OBP-401 at an MOI of 0.1 PFU/cell and the culture medium was replaced with freshly prepared medium containing docetaxel at 10 nM at 2 hr after infection, and photomicrographs were taken every day at a magnification of ×100.

In vitro *replication assay*

H1299 and SW620 cells were seeded on 25-cm^2 flasks at 5×10^4 cells at 48 hr before infection. Cells were infected with OBP-401 at an MOI of 0.1 PFU/cell and a fresh medium containing docetaxel at 10 nM was added 24 hr later. Alternatively, cells were pretreated with 10 nM of docetaxel for 24 hr, infected with 0.1 PFU/cell of OBP-401 for 2 hr, and then cultured in the presence of 10 nM of docetaxel following the removal of viruses. The cells were incubated at 37°C, trypsinized and harvested for intracellular replication analysis at 2, 12, 24, 36, 48 and 60 hr. The supernatants of H1299 and SW620 cells were also harvested for viral progenies release analysis at the indicated time points over 120 hr. DNA purification was performed using QIAmp DNA mini kit (Qiagen Inc., Valencia, CA). The E1A DNA copy number was determined by quantitative real time PCR, using a LightCycler instrument and LightCycler-DNA Master SYBR Green I (Roche Diagnostics).

In vivo *human tumor model*

H1299 cells (1×10^7 cells/mouse) were injected subcutaneously into the flank of 5–6-week-old female BALB/c *nu/nu* mice and permitted to grow to ~5–10 mm in diameter. At that time, the mice were randomly assigned into 4 groups, and a 50-μl solution containing OBP-401, at a dose of 1×10^7 PFU/body or PBS was injected into the tumor. Simultaneously, each mouse received an intraperitoneal injection of 100 μl of docetaxel at a dose of 12.5 mg/kg every 2 days starting at day 1. The perpendicular diameter of each tumor was measured every 3 days, and tumor volume was calculated using the following formula: tumor volume (mm^3) = $a \times b^2 \times 0.5$, where a is the longest diameter, b is the shortest diameter and 0.5 is a constant to calculate the volume of an ellipsoid. The experimental protocol was approved by the Ethics Review Committee for Animal Experimentation of Okayama University School of Medicine.

Histopathological study

Mice were sacrificed 6 days after the final dose of OBP-401 and docetaxel, and histochemical examination was performed. Tumors and liver tissues were fixed in 10% Formalin, embedded in paraffin, and then cut into 4-μm thick sections. Liver tissue samples and tumor sections were stained with hematoxylin and eosin.

Results

Antitumor efficacy of OBP-401 plus docetaxel in human cancer cell lines in vitro

The tumor-specific replication-competent GFP-expressing adenovirus OBP-401 was constructed by inserting the GFP gene under the control of the CMV promoter at the deleted E3 region of

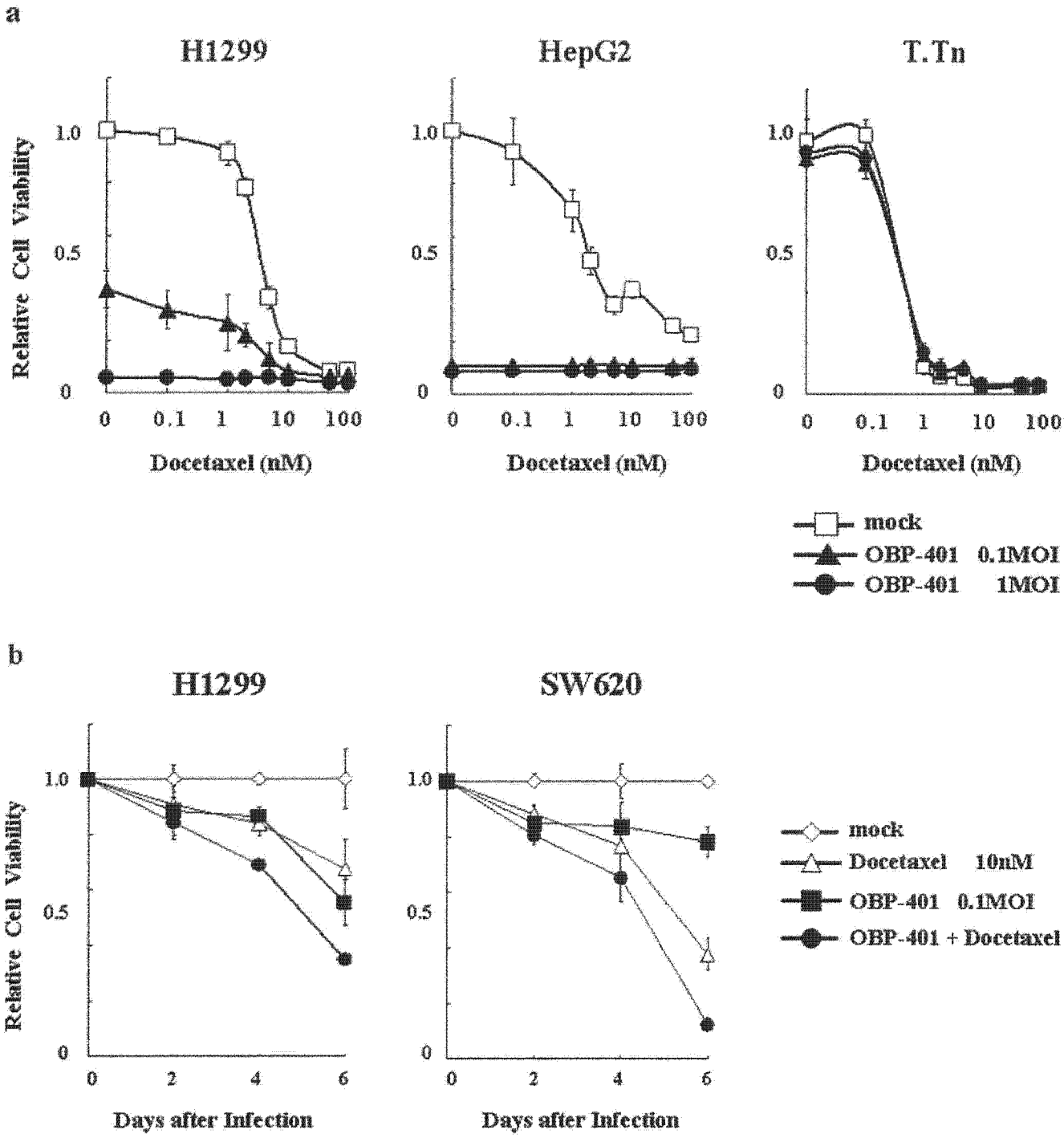

FIGURE 2 – Combination effect of OBP-401 and docetaxel on human cancer cell lines. (*a*) Cells were infected with 0.1 or 1 MOI of OBP-401, and then exposed to docetaxel at the indicated concentrations at 24 hr after infection. Cell viability was assessed by XTT assay at 5 days after OBP-401 infection. The results of H1299 (lung), HepG2 (liver) and T.Tn (esophagus) cells were shown as representative of 10 cell lines. Bars, standard deviation (SD). (*b*) Time course of combined effect of OBP-401 plus docetaxel on H1299 and SW620 cells. Cells were treated with 0.1 MOI of OBP-401, 10 nM of docetaxel, or a combination of both, and cell killing efficacy was evaluated by XTT assay over 6 days. Docetaxel was added to the medium 24 hr after OBP-401 infection (day 1).

the telomerase-specific replication-selective type 5 adenovirus OBP-301 (Fig. 1). To examine the potential interaction between OBP-401 and docetaxel *in vitro*, we first evaluated the effect of the 2 modalities at various doses in 10 human cancer cell lines originating from different organs (lung [H1299, A549 and H226Br], colon [SW620 and DLD-1], esophagus [TE8 and T.Tn], stomach [MKN28], liver [HepG2] and prostate [LNCaP]). The cell viability with 3 different doses of OBP-401 and 8 doses of docetaxel was assessed by XTT assay 5 days after treatment. To optimize the experimental design, the concentrations of docetaxel that resulted in 0–100% cell kill when given alone were chosen. The addition of 0.1 MOI of OBP-401 increased the cell killing ac-

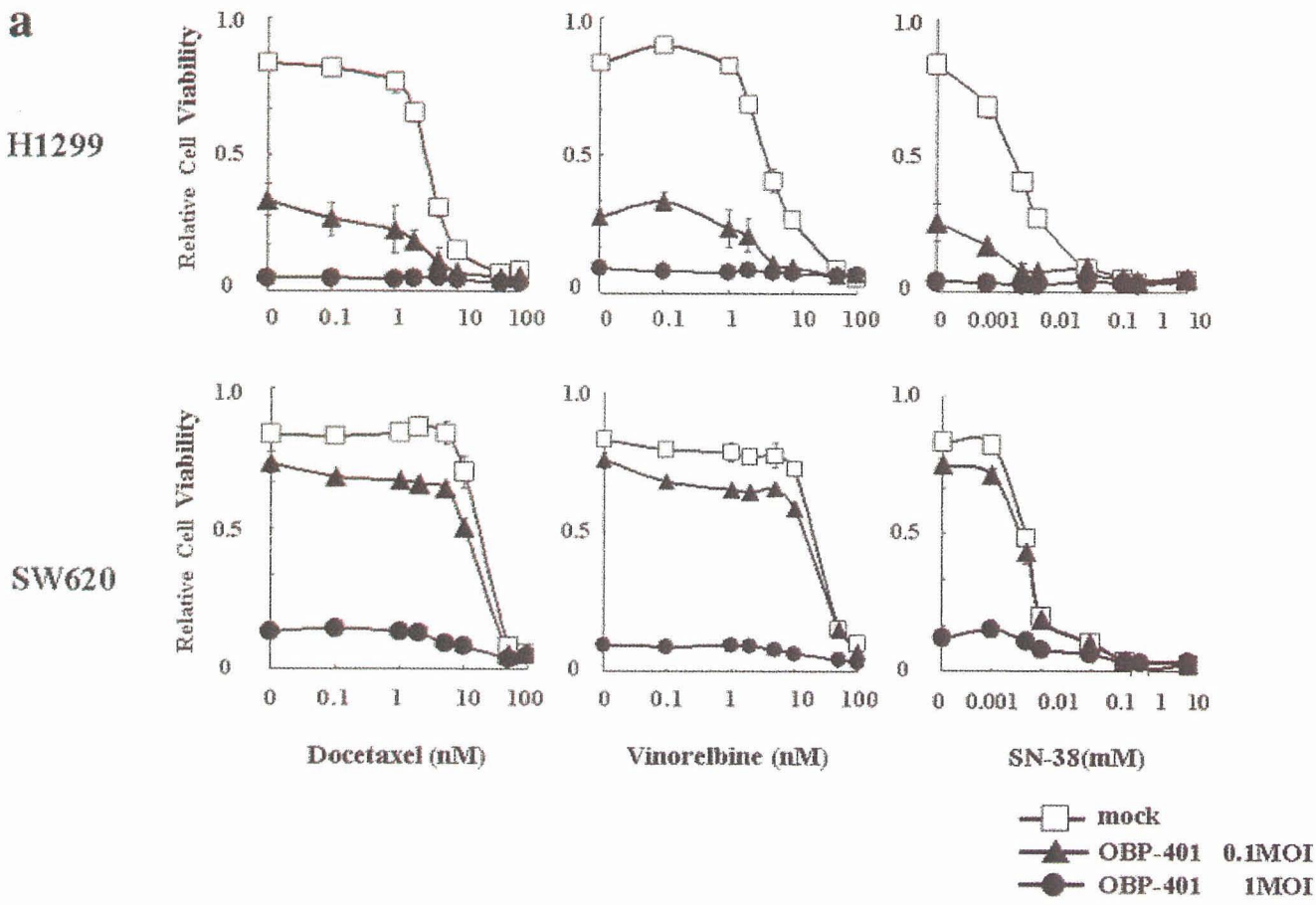

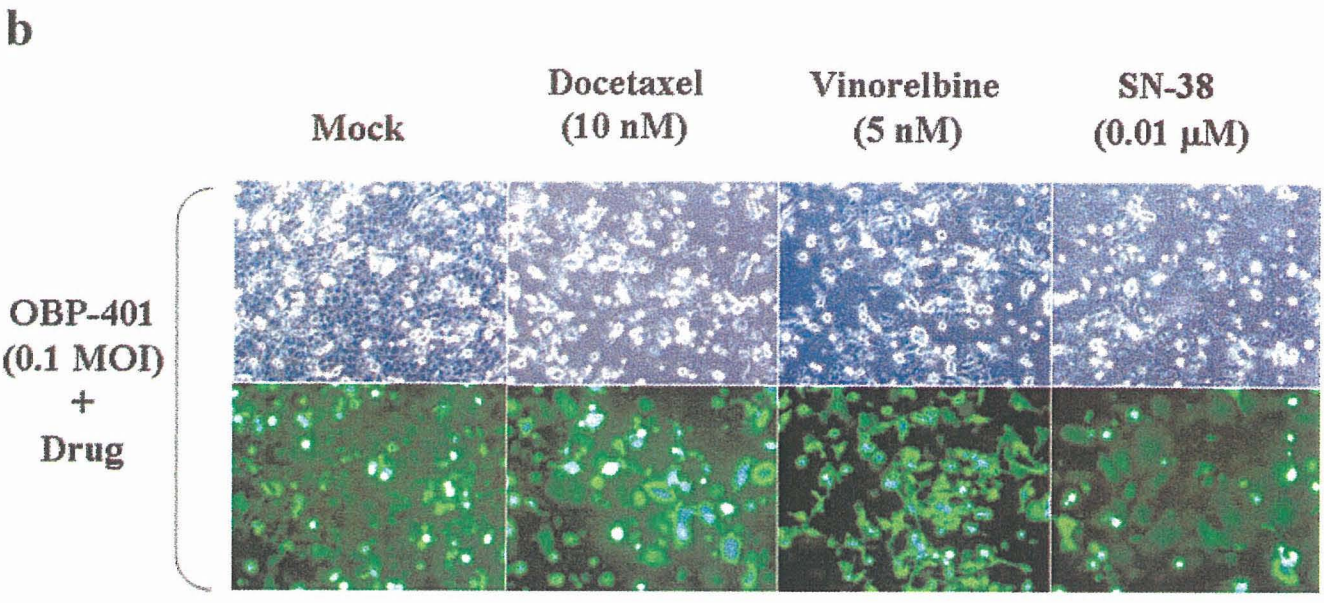

FIGURE 3 – Combination efficacy of OBP-401 with other chemotherapeutic agents, the topoisomerase I inhibitor SN-38 (active irinotecan metabolite) and microtubule-interfering agent vinorelbine. (*a*) H1299 and SW620 cells were infected with 0.1 or 1 MOI of OBP-401, and then exposed to docetaxel, vinorelbine or SN-38 at the indicated concentrations 24 hr after infection. Cell viability was assessed by XTT assay 5 days after OBP-401 infection. Data are mean ± SD. (*b*) H1299 cells were treated with OBP-401 alone or in combination with drugs (docetaxel [10 nM], vinorelbine [5 nM] or SN-38 [0.01 μM]) according to the schedule described above, and photographed 4 days after OBP-401 infection. Upper panel: phase-contrast images; lower panel: fluorescent images for GFP expression. ×100 magnification.

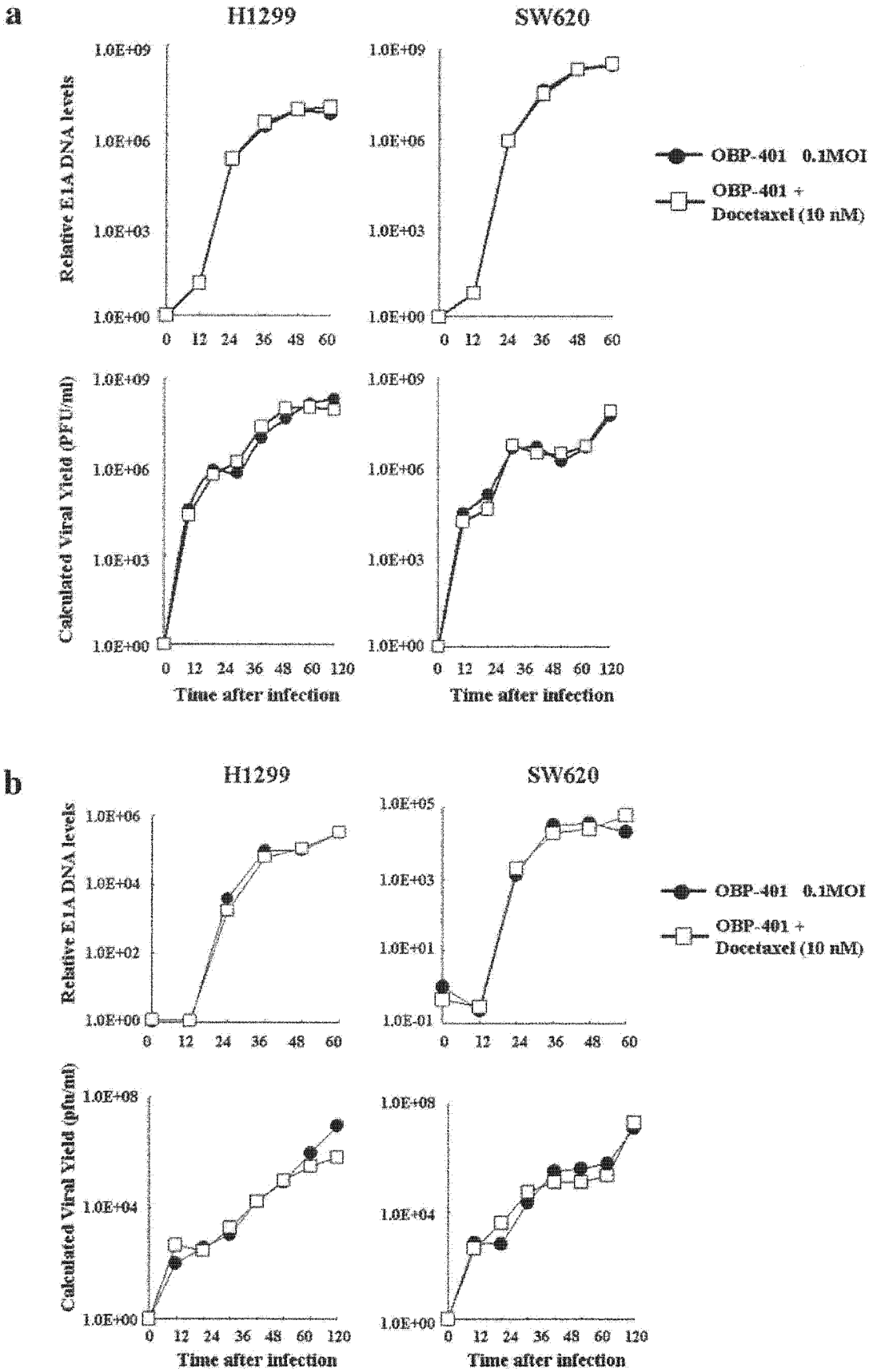

FIGURE 4 – Assessment of viral DNA replication in H1299 and SW620 cells. (*a*) Cells were infected with OBP-401 at an MOI of 0.1 for 2 hr. Following the removal of virus inocula, the cells were further incubated with docetaxel for indicated periods of time. (*b*) Alternatively, cells were treated with docetaxel, followed by 0.1 MOI of OBP-401 infection 24 hr later. Cells (upper panels) and culture supernatants (lower panels) were then subjected to real-time quantitative PCR assay. The amounts of viral E1A copy number are defined as the fold increase for each sample relative to that at 2 hr (2 hr equals 1).

tivity of docetaxel, especially at low concentrations (<10 nM), in most of cell lines, including H1299, SW620, DLD-1, A549, MKN28 and TE8, although OBP-401 at an MOI of 1 alone showed an apparent cell killing activity in these cell lines. In contrast, the effect of the combination was unclear in HepG2, LNCaP, H226Br and T.Tn cell lines, since HepG2 and LNCaP cells were too sensitive and H226Br and T.Tn cells were too resistant to OBP-401. The representative dose–response curves on H1299, HepG2 and T.Tn cells were shown in Figure 2*a*.

We next performed a time-course analysis of the cell killing effect of 0.1 MOI of OBP-401 combined with 10 nM of docetaxel in H1299 and SW620 cells. The viability of cells treated with both agents was consistently lower than that of cells treated with either drug alone over 6 days (Fig. 2*b*). To determine whether the timing of administration of the tested agents affected the combined cytotoxic effect, H1299 and SW620 cells were treated with docetaxel 24 hr before infection, after infection or synchronously with OBP-401. The results showed no apparent differences in the cytotoxic activity of the schedules (data not shown).

Effect of vinorelbine and SN-38 on OBP-401-mediated antitumor activity in human cancer cells in vitro

We also examined the interactive effects of OBP-401 when combined with other chemotherapeutic agents such as the topoisomerase 1 inhibitor, SN-38 (the active irinotecan metabolite), and a microtubule-interfering agent, vinorelbine, in H1299 and SW620 cells. As shown in Figure 3*a*, the profile of the cytotoxic effects of OBP-401 plus vinorelbine was similar to that of OBP-401 plus docetaxel, whereas the range of combination effectiveness was narrow when combined with SN-38. The combined effect of OBP-401 plus SN38 diminished with the use of high concentrations of SN38, suggesting that inhibition of DNA synthesis may be deleterious for viral replication.

One of the advantages of OBP-401 over OBP-301 is that the viral distribution of OBP-401 can be monitored by GFP fluorescence. With time, infected cells fluoresce in green color, and they expand, float and gather in the center of the well. To confirm visually the viral replication and spread following OBP-401 application, H1299 cells were treated with OBP-401 at an MOI of 0.1 plus 10 nM docetaxel, 5 nM vinorelbine or 0.01 μM SN-38. Phase-contrast images demonstrated growth of H1299 cells to subconfluence in the presence of the chemotherapeutic drugs alone 4 days after treatment, whereas a rapid loss of viability due to massive cell death, as evidenced by ballooning and floating cells, was evident when combined with OBP-401 infection (Fig. 3*b*). A strong and persistent GFP fluorescence expression, which indicates the viral replication and spread into the neighboring tumor cells, was detectable in H1299 cells infected with OBP-401 under a fluorescence microscope even in the presence of chemotherapeutic drugs. The signal intensity of cells treated with OBP-401 plus docetaxel or vinorelbine was equivalent to that of cells infected with OBP-401 alone, whereas the levels of GFP expression was relatively weak in cells treated with OBP-401 and SN-38.

Effect of docetaxel on OBP-401 virus replication in human cancer cells in vitro

We next examined the effect of docetaxel on replication and release of viral progenies by quantitative real-time PCR analysis. H1299 and SW620 cells were infected with OBP-401 at an MOI of 0.1 for 24 hr, and then treated with 10 nM of docetaxel. Alternatively, cells were treated with docetaxel at 10 nM, and then infected with 0.1 MOI of OBP-401 24 hr later. The cells and supernatants were harvested at indicated time points over 60 or 120 hr after infection, and extracted DNA was subjected to the assay. As shown in Figure 4, the increases of intracellular and supernatant viral copy numbers of OBP-401 by 5–9 orders of magnitude were consistent with and without docetaxel over time in both treatment regimens. A plateau was reached at ~48 hr after infection. These results suggest that docetaxel does not interfere with OBP-401 replication.

Antitumor effect of OBP-401 plus docetaxel in human tumor xenografts

Finally, we assessed the therapeutic efficacy of OBP-401 in combination with docetaxel against H1299 human cells *in vivo*. H1299 cells were implanted as xenografts into the hind flank of *nu/nu* mice. Mice bearing palpable H1299 tumors measuring 5–10 mm in diameter received simultaneous treatment of intratumoral injection of either 10^7 PFU of OBP-401 or PBS plus intraperitoneal administration of either 12.5 mg/kg docetaxel or PBS every 2 days for 3 cycles starting at day 1. As shown in Figure 5, administration of OBP-401 or docetaxel resulted in a significant tumor growth suppression compared with mock-treated tumors at 27 days after initiation of treatment ($p < 0.05$). However, the combination of OBP-401 plus docetaxel produced a more profound and significant inhibition of tumor growth compared with mice treated with either modality ($p < 0.05$), and mock-treated tumors ($p < 0.01$). Intratumoral injection of a replication-deficient adenovirus with or without systemic administration of docetaxel had no apparent effect on the growth of H1299 tumors (data not shown).

To investigate the mechanism of action of these therapies and their influence on other body tissues, mice were sacrificed 6 days after the last administration of 10^7 PFU of OBP-401 and 12.5 mg/kg docetaxel. Fluorescent images of frozen sections demonstrated that intratumorally administered OBP-401 spread throughout the tumors whether combined with docetaxel or not, whereas no GFP-expressing cells were detected in the liver tissues (Fig. 6*a*). The broad virus distribution in the tumor was also confirmed by immunohistochemical staining of adenoviral hexon protein (data not shown). Histopathological analysis revealed massive degeneration of tissues, especially in the central portions of tumors injected with OBP-401, but not in those treated with docetaxel alone (Fig. 6*b*). In contrast, analysis of liver sections from mice treated with OBP-401 demonstrated no histological evidence of hepatocellular damage.

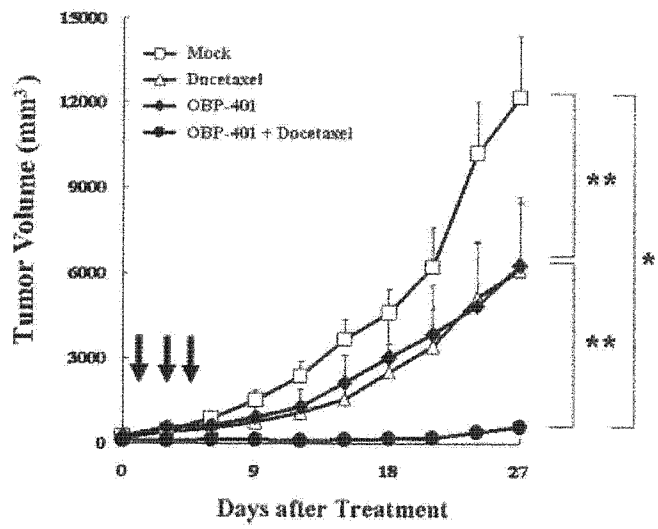

FIGURE 5 – Antitumor effects of intratumorally injected OBP-401and intraperitoneally administered docetaxel against established flank H1299 xenograft tumors in *nu/nu* mice. H1299 tumor cells (1×10^7 cells/each) were subcutaneously injected into the right flank of mice. OBP-401 (1×10^7 PFU/body) and docetaxel (12.5 mg/kg) were administered intratumorally and intraperitoneally, respectively, for 3 cycles every 2 days. PBS was used as the control. Six mice were used for each group. Tumor growth was expressed by tumor mean volume ± SE. Statistical significance was defined as $p < 0.01$ (*) or $p < 0.05$ (**) (Student's *t*-test). Arrows, day of treatment.

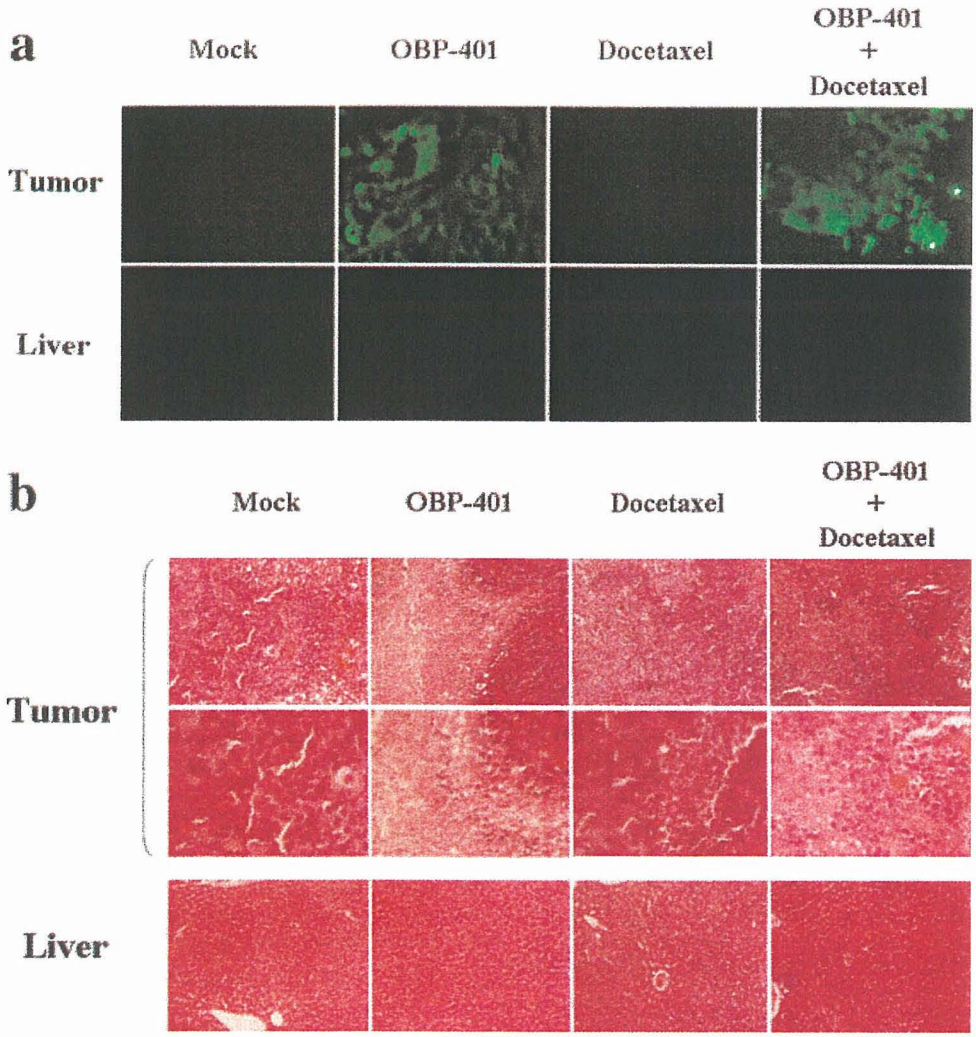

FIGURE 6 – Mice bearing H1299 xenografts were treated as described in the legend for Figure 5. Tumor and liver sections were then obtained 6 days after final administration of OBP-401 and docetaxel. (*a*) Fluorescent photomicrographs showing GFP expression in H1299 tumors and the liver. Magnification, ×200. (*b*) Paraffin sections of tumors and the liver were stained with hematoxylin and eosin. Tumors: (upper panel) magnification, ×200, (lower panel) magnification, ×400. Livers: magnification, ×200.

Discussion

Treatment of advanced human cancer has not significantly improved clinical outcome. Replication-competent oncolytic adenovirus is promising as a novel anticancer therapy.[5–9] In our laboratory, the tumor-specific replication-selective adenovirus, named Telomelysin or OBP-301, has been shown to be effective against human cancers.[10–12] This virus was genetically designed to replicate under the control of hTERT promoter specifically in tumor cells, causing specific "oncolysis." Therefore, OBP-301 did not cause significant toxicity in normal human cell lines, as shown in our previous report.[10–12] In humans, telomerase activity is found in only few cell types like stem and germ-line cells. Thus, there is concern that these cells might be permissive for OBP-301 replication; these cells, however, are not of epithelial origin and are therefore extremely difficult to be targeted with adenoviral vectors.[20]

Preclinical studies provided experimental evidence for effective killing of cancer cells by oncolytic viruses.[5–9] In animal models, however, established xenograft tumors are rarely eliminated despite existence of persistently high viral titers within the tumor. Total elimination of solid tumor requires higher doses of oncolytic viruses, which might be toxic or lethal. In a report of clinical trial of ONYX-015, no clinical benefit was noted in the majority of patients, despite the encouraging biological activity.[21] Tumor progression was rapid in most patients, even though substantial necrosis was noted in the tumors after treatment.[22,23] Therefore, we searched for new modalities and opted to evaluate chemovirotherapy, composed of oncolytic virotherapy combined with low-dose chemotherapeutic agent. Combination of 2 agents may allow the use of reduced dosage of each agent, and reduce the likelihood of adverse effects.

The efficacy of virotherapy combined with anticancer drugs has been reported previously in preclinical studies.[24–26] A replication-selective adenovirus, ONYX-015, combined with 5-fluorouracil or CDDP produced greater effect than each individual modality and prolonged survival.[24,25] Furthermore, synergistic efficacy was also observed in the combination of a tumor-specific HSV mutant (HSV-1716) with chemotherapeutic agents in human non-small cell lung cancer.[26] However, care should be taken when using a combination of anti-DNA synthetic agents because they might have deleterious effects on viral replication. Because adenoviral E1A directs the progression cells from G1/G0 phase to S phase to optimize viral DNA replication, these agents could harm this function by inhibiting DNA synthesis.

Taxanes are novel antimicrotubule agents that promote the assembly of microtubules from tubulin dimers and stabilize microtubules by preventing depolymerization. This stability results in the inhibition of the normal dynamic reorganization of the microtubule network, which is essential for vital interphase and mitotic cellular functions, resulting in cell arrest in G2 and M phases.[17,18] Apoptotic cell death is induced subsequently, but this does not inhibit DNA synthesis of host cells. Therefore, taxanes are promising for combination with virotherapy. It was reported previously

that paclitaxel had a synergistic or an additive effect in several cancer models when combined with Ad-mediated p53 gene therapy.[27] It has been also demonstrated that CV787, a prostate cancer-specific adenovirus, exhibited synergistic antitumor effect when combined with paclitaxel or docetaxel.[28]

OBP-401, containing the hTERT promoter-driven replication cassette and the GFP gene driven by the CMV promoter, was developed to monitor replication and visualize distribution of virus (Fig. 1). As GFP was originally identified from the jellyfish *Aequorea victoria*, and broadly used for molecular and functional monitoring of cellular processes, GFP is considered nontoxic to normal tissues.[11,29] We demonstrated that OBP-401 effectively destroyed a variety of human cancer cells *in vitro*, and that such effect was markedly enhanced when it was combined with docetaxel (Figs. 2 and 3). Quantitative real-time PCR analysis showed that intracellular amplification of OBP-401 and viral release into the culture supernatants were not affected by docetaxel (Fig. 4), suggesting that the latter did not alter viral replication *in vitro*. Low-dose taxanes induced G2/M arrest without inhibiting DNA synthesis, which in turn led to apoptosis, whereas OBP-401 infection had no effect on cell cycle distribution as demonstrated in flow cytometric analysis (data not shown). These results indicate that the antitumor machinery is different between docetaxel and OBP-401. Indeed, nuclear morphology of cells infected with OBP-401 was distinct from apoptosis, which is characterized by chromosome condensation and nuclear shrinkage and fragmentation (data not shown). Moreover, apoptosis in mammalian cells is mediated by a family of cysteine proteases known as caspases, which are the executioners of apoptosis and essential for the disassembly of the cell. Western blot analyses demonstrated no changes in procaspase-3 levels and no expression of cleaved form of caspase-3 in H1299 cells infected with OBP-401 (data not shown).

There is evidence that changes in the expression of microtubule-associated protein 4 (MAP4) affect the sensitivity to antimicrotubule drugs. Expression of MAP4 is transcriptionally repressed by wild-type p53. Increased expression of MAP4, which occurs when p53 is transcriptionally inactive, augments microtubule polymerization, taxanes binding and sensitivity to taxanes, which stabilizes polymerized microtubules.[30] Our preliminary experiments, however, demonstrated that OBP-401 infection did not affect the expression of MAP4 in human cancer cells (data not shown). Thus, the mechanism of combination effect of OBP-401 and docetaxel is still unclear.

Our *in vitro* data raise the possibility that docetaxel-mediated apoptosis and OBP-401-mediated oncolysis coexisted; these agents did not interfere with mutually and individually induced antitumor efficacy. In fact, the antitumor effect of the combination therapy was likely additive *in vitro*. To determine whether the interaction between the 2 drugs exhibited synergistic or additive cytotoxic effects, the data from a series of dose–response curves was examined by constructing isobolograms. Isobologram analysis indicated that the combination was less than synergistic across all dose levels tested (data not shown). In contrast, interestingly, intratumoral injection of OBP-401 combined with systemic administration of docetaxel induced a more pronounced inhibition of the growth of H1299 tumor xenografts over a long period of time (Fig. 5). Therefore, there might be some particular interactions between OBP-401 and docetaxel to produce a synergistic effect *in vivo*. It has been reported that metronomic chemotherapy, which refers to the chronic administration of comparatively low doses of cytotoxic drugs at close, regular intervals has an antiangiogenic basis.[31] Like our approach, the potent antiangiogenic capacity of drug administered in a metronomic fashion finds favor in a number of *in vivo* preclinical studies; to prove this efficacy with *in vitro* experiments is, however, technically difficult. There are some possible explanations for the superior *in vivo* antitumor activity in our experiments. Systemically administered docetaxel may attack the vascular endothelial cells in the tumor site, which in turn can block the escape of locally injected OBP-401 into the blood circulation. Another possibility is that OBP-401 itself may inhibit the vascular supply by killing endothelial cells. Virtually, the exact mechanism of this *in vivo* combination effect needs further examination.

In summary, our data demonstrated that the combination of OBP-401 and docetaxel efficiently inhibited human cancer cell growth both *in vitro* and *in vivo*, an outcome that has important implications for tumor-specific oncolytic chemovirotherapies for human cancers.

References

1. Blackburn EH. Structure and function of telomeres. Nature (Lond.) 1991;350:569–73.
2. Kim NW, Piatyszek MA, Prowse KR, Harley CB, West MD, Ho PL, Coviello GM, Wright WE, Weinrich SL, Shay JW. Specific association of human telomerase activity with immortal cells and cancer. Science 1994;266:2011–5.
3. Shay JW, Wright WE. Telomerase activity in human cancer. Curr Opin Oncol 1996;8:66–71.
4. Nakayama J, Tahara H, Tahara E, Saito M, Ito K, Nakamura H, Nakanishi T, Tahara E, Ide T, Ishikawa F. Telomerase activation by hTRT in human normal fibroblasts and hepatocellular carcinomas. Nat Genet 1998;18:65–8.
5. Bischoff JR, Kirn DH, Williams A, Heise C, Horn S, Muna M, Ng L, Nye JA, Sampson-Johannes A, Fattaey A, McCormick F. An adenovirus mutant that replicates selectively in p53-deficient human tumor cells. Science 1996;274:373–6.
6. Rodriguez R, Schuur ER, Lim HY, Henderson GA, Simons JW, Henderson DR. Prostate attenuated replication competent adenovirus (ARCA) CN706: a selective cytotoxic for prostate-specific antigen-positive prostate cancer cells. Cancer Res 1997;57:2559–63.
7. Tsukuda K, Wiewrodt R, Molnar-Kimber K, Jovanovic VP, Amin KM. An E2F-responsive replication-selective adenovirus targeted to the defective cell cycle in cancer cells: potent antitumoral efficacy but no toxicity to normal cell. Cancer Res 2002;62:3438–47.
8. Li Y, Yu DC, Chen Y, Amin P, Zhang H, Nguyen N, Henderson DR. A hepatocellular carcinoma-specific adenovirus variant, CV890, eliminates distant human liver tumors in combination with doxorubicin. Cancer Res 2001;61:6428–36.
9. Kirn D, Martuza RL, Zwiebel J. Replication-selective virotherapy for cancer: biological principles, risk management and future directions. Nat Med 2001;7:781–7.
10. Kawashima T, Kagawa S, Kobayashi N, Shirakiya Y, Umeoka T, Teraishi F, Taki M, Kyo S, Tanaka N, Fujiwara T. Telomerase-specific replication-selective virotherapy for human cancer. Clin Cancer Res 2004;10:285–92.
11. Umeoka T, Kawashima T, Kagawa S, Teraishi F, Taki M, Nishizaki M, Kyo S, Nagai K, Urata Y, Tanaka N, Fujiwara T. Visualization of intrathoracically disseminated solid tumors in mice with optical imaging by telomerase-specific amplification of a transferred green fluorescent protein gene. Cancer Res 2004;64:6259–65.
12. Taki M, Kagawa S, Nishizaki M, Mizuguchi H, Hayakawa T, Kyo S, Nagai K, Urata Y, Tanaka N, Fujiwara T. Enhanced oncolysis by a tropism-modified telomerase-specific replication-selective adenoviral agent OBP-405 ('Telomelysin-RGD'). Oncogene 2005;24:3130–40.
13. Khuri FR, Nemunaitis J, Ganly I, Arseneau J, Tannock IF, Romel L, Gore M, Ironside J, MacDougall RH, Heise C, Randlev B, Gillenwater AM, et al. A controlled trial of intratumoral ONYX-015, a selectively-replicating adenovirus, in combination with cisplatin and 5-fluorouracil in patients with recurrent head and neck cancer. Nat Med 2000;6:879–85.
14. Reid T, Galanis E, Abbruzzese J, Sze D, Wein LM, Andrews J, Randlev B, Heise C, Uprichard M, Hatfield M, Rome L, Rubin J, et al. Hepatic arterial infusion of a replication-selective oncolytic adenovirus (dl1520): phase II viral, immunologic, and clinical endpoints. Cancer Res 2002;62:6070–9.
15. Hecht JR, Bedford R, Abbruzzese JL, Lahoti S, Reid TR, Soetikno RM, Kirn DH, Freeman SM. A phase I/II trial of intratumoral endoscopic ultrasound injection of ONYX-015 with intravenous gemcitabine in unresectable pancreatic carcinoma. Clin Cancer Res 2003;9:555–61.
16. Galanis E, Okuno SH, Nascimento AG, Lewis BD, Lee RA, Oliveira AM, Sloan JA, Atherton P, Edmonson JH, Erlichman C, Randlev B, Wang Q, et al. Phase I-II trial of ONYX-015 in combination with MAP chemotherapy in patients with advanced sarcomas. Gene Ther 2005;12:437–45.

17. Dumontet C, Sikic B. Mechanisms of action of and resistance to antitubulin agents: microtubule dynamics, drug transport, and cell death. J Clin Oncol 1999;17:1061–70.
18. Jordan M, Toso R, Thrower D, Wilson L. Mechanism of mitotic block and inhibition of cell proliferation by taxol at low concentrations. Proc Natl Acad Sci USA 1993;90:9552–6.
19. Tsunemitsu Y, Kagawa S, Tokunaga N, Otani S, Umeoka T, Roth JA, Fang B, Tanaka N, Fujiwara T. Molecular therapy for peritoneal dissemination of xenotransplanted human MKN-45 gastric cancer cells with adenovirus mediated Bax gene transfer. Gut 2004;53:554–60.
20. Peters AH, Drumm J, Ferrell C, Roth DA, Roth DM, McCaman M, Novak PL, Friedman J, Engler R, Braun RE. Absence of germline infection in male mice following intraventricular injection of adenovirus. Mol Ther 2001;4:603–13.
21. Nemunaitis J, Ganly I, Khuri F, James Arseneau J, Kuhn J, McCarty T, Landers S, Maples P, Romel L, Randlev B, Reid T, Kaye S, et al. Selective replication and oncolysis in p53 mutant tumors with ONYX-015, an E1B-55kD gene-deleted adenovirus, in patients with advanced head and neck cancer: a phase II trial. Cancer Res 2000; 60:6359–66.
22. Jacobs C, Lyman G, Velez-Garcia E, Sridhar KS, Knoght W, Hochster H, Goodnough LT, Mortimer JE, Einhorn LH, Schacter LA. Phase III randomized study comparing cisplatin and fluorouracil as single agents and in combination for advanced squamous cell carcinoma of the head and neck. J Clin Oncol 1992;10:257–63.
23. Vokes EE. Chemotherapy and integrated treatment approaches in head and neck cancer. Curr Opin Oncol 1991;3:529–34.
24. Heise C, Sampson-Johannes A, Williams A, McCormick F, Von Hoff DD, Kirn DH. ONYX-015, an E1B gene-attenuated adenovirus, causes tumor-specific cytolysis and antitumoral efficacy that can be augmented by standard chemotherapeutic agents. Nat Med 1997;3: 639–45.
25. You L, Yang CT, Jablons DM. ONYX-015 works synergistically with chemotherapy in lung cancer cell lines and primary cultures freshly made from lung cancer patients. Cancer Res 2000;60:1009–13.
26. Toyoizumi T, Mick R, Abbas AE, Kang EH, Kaiser LR, Molnar-Kimber KL. Combined therapy with chemotherapeutic agents and herpes simplex virus type 1 ICP34.5 mutant (HSV-1716) in human non-small cell lung cancer. Hum Gene Ther 1999;10:3013–29.
27. Nielsen LL, Lipari P, Dell J, Gurnani M, Hajian G. Adenovirus-mediated p53 gene therapy and paclitaxel have synergistic efficacy in models of human head and neck, ovarian, prostate, and breast cancer. Clin Cancer Res 1998;4:835–46.
28. Yu DC, Chen Y, Dilley J, Li Y, Embry M, Zhang H, Nguyen N, Amin P, Oh J, Henderson DR. Antitumor synergy of CV787, a prostate cancer-specific adenovirus, and paclitaxel and docetaxel. Cancer Res 2001;61:517–25.
29. Richards HA, Han CT, Hopkins RG, Failla ML, Ward WW, Stewart CN. Safety assessment of recombinant green fluorescent protein orally administered to weaned rats. J Nutr 2003;133:1909–12.
30. Zhang CC, Yang JM, Bash-Babula J, White E, Murphy M, Levine AJ, Hait WN. DNA damage increases sensitivity to vinca alkaloids and decreases sensitivity to taxanes through p53-dependent repression of microtubule-associated protein 4. Cancer Res 1999;59:3663–70.
31. Shaked Y, Emmenegger U, Francia G, Chen L, Lee CR, Man S, Paraghamian A, Ben-David Y, Kerbel RS. Low-dose metronomic combined with intermittent bolus-dose cyclophosphamide is an effective long-term chemotherapy treatment strategy. Cancer Res 2005;65: 7045–51.

nature medicine

In vivo imaging of lymph node metastasis with telomerase-specific replication-selective adenovirus

Hiroyuki Kishimoto[1,2], Toru Kojima[1,2], Yuichi Watanabe[1,3], Shunsuke Kagawa[1,2], Toshiya Fujiwara[1,2], Futoshi Uno[1,2], Fuminori Teraishi[1,2], Satoru Kyo[4], Hiroyuki Mizuguchi[5], Yuuri Hashimoto[3], Yasuo Urata[3], Noriaki Tanaka[1] & Toshiyoshi Fujiwara[1,2]

Currently available methods for detection of tumors *in vivo* such as computed tomography and magnetic resonance imaging are not specific for tumors. Here we describe a new approach for visualizing tumors whose fluorescence can be detected using telomerase-specific replication-competent adenovirus expressing green fluorescent protein (GFP) (OBP-401). OBP-401 contains the replication cassette, in which the human telomerase reverse transcriptase (hTERT) promoter drives expression of *E1* genes, and the *GFP* gene for monitoring viral replication. When OBP-401 was intratumorally injected into HT29 tumors orthotopically implanted into the rectum in BALB/c *nu/nu* mice, para-aortic lymph node metastasis could be visualized at laparotomy under a three-chip color cooled charged-coupled device camera. Our results indicate that OBP-401 causes viral spread into the regional lymphatic area and selectively replicates in neoplastic lesions, resulting in GFP expression in metastatic lymph nodes. This technology is adaptable to detect lymph node metastasis *in vivo* as a preclinical model of surgical navigation.

Medical imaging techniques have become an essential aspect of cancer diagnosis, detection, and treatment monitoring. Advances and improvements in the major imaging modalities such as computed tomography, magnetic resonance imaging and ultrasound techniques have increased the sensitivity of visualizing tumors and their metastases in the body[1,2]. A limiting factor of these techniques is, however, the inability to specifically identify malignant tissues. Positron emission tomography with the glucose analog ^{18}F-2-deoxy-D-glucose is the first molecular imaging technique that has been widely applied for cancer imaging in clinical settings[3]. Although ^{18}F-2-deoxy-D-glucose–positron emission tomography has high detection sensitivity, it has some limitations such as the difficulty in distinguishing between proliferating tumor cells and inflammation and the inability in using it for real-time detection of tumor tissues. A relatively inexpensive, robust and straightforward way of defining the location and area of tumors *in vivo* would greatly aid the treatment of human cancer, especially for surgical procedures. In particular, if tumors too small for direct visual detection and therefore not detectable by direct inspection could be imaged *in situ*, surgeons could excise such tumors precisely with appropriate surgical margins.

Sentinel lymph node (SLN) mapping is a minimally invasive procedure and widely used in the management of patients with cutaneous melanoma or breast cancer without clinical evidence of nodal metastases[4,5]. The technique assumes that early lymphatic metastases, if present, are always found first within the SLN, the first tumor-draining lymph node. A SLN free of tumor cells would therefore predict the absence of metastatic disease in the rest of the tumor-draining lymph node basin, which indicates that intensive lymphadenectomy is unlikely to benefit those patients. Several studies have validated this assumption; the sensitivity of intraoperative frozen-section analysis for detection of nodal metastases, however, is relatively low, and high false-negative rates have been reported[6–9]. In addition, thicker primary and larger SLN tumor size has been shown to be predictive of non-SLN metastasis, presumably because of the altered lymphatic drainage routes. These findings raise doubt about the applicability of this technique in widespread surgical practice; therefore, several different approaches have been taken to directly label tumor cells to visualize and track them *in vivo*.

The GFP, which was originally identified from the jellyfish *Aequorea victoria*, is an attractive molecular marker for imaging in live tissues because of the relatively noninvasive nature of fluorescence[10–15]. We previously demonstrated a real-time fluorescence optical imaging of pleural dissemination of human non-small-cell lung cancer cells in an orthotopic mouse model using tumor-specific replication-competent adenovirus (OBP-301, Telomelysin)[16,17] in combination with replication-deficient adenovirus expressing *GFP* (Ad-*GFP*)[18]. In the present study we additionally modified OBP-301 to contain the *GFP* gene driven by the cytomegalovirus (CMV) promoter for monitoring viral replication. The resultant adenovirus, termed OBP-401, efficiently labeled tumor cells with green fluorescence *in vitro* and *in vivo*. The results showed that injection of OBP-401 into primary tumors allows its lymphatic spread, which in turn induces viral replication in

[1]Division of Surgical Oncology, Department of Surgery, Okayama University Graduate School of Medicine, Dentistry and Pharmaceutical Sciences, 2-5-1 Shikata-cho, Okayama 700-8558, Japan. [2]Center for Gene and Cell Therapy, Okayama University Hospital, 2-5-1 Shikata-cho, Okayama 700-8558, Japan. [3]Oncolys BioPharma, Inc., 3-16-33 Roppongi, Minato-ku, Tokyo 106-0032, Japan. [4]Department of Obstetrics and Gynecology, Kanazawa University School of Medicine, 13-1 Takara-machi, Kanazawa 920-8641, Japan. [5]Laboratory of Gene Transfer and Regulation, National Institute of Biomedical Innovation, 7-6-8 Saito-Asagi, Ibaraki, Osaka 567-0085, Japan. Correspondence should be addressed to T.F. (toshi_f@md.okayama-u.ac.jp).

Received 9 February; accepted 3 April; published online 1 October 2006; doi:10.1038/nm1404